

AD-A034 007

AIR FORCE INST OF TECH WRIGHT-PATTERSON AFB OHIO SCH--ETC F/6 20/12  
ION IMPLANTATION IMPURITY ANALYSIS BY GLOW DISCHARGE OPTICAL SP--ETC(U)  
DEC 76 D S HAKE

UNCLASSIFIED

SEP/PH/760-5

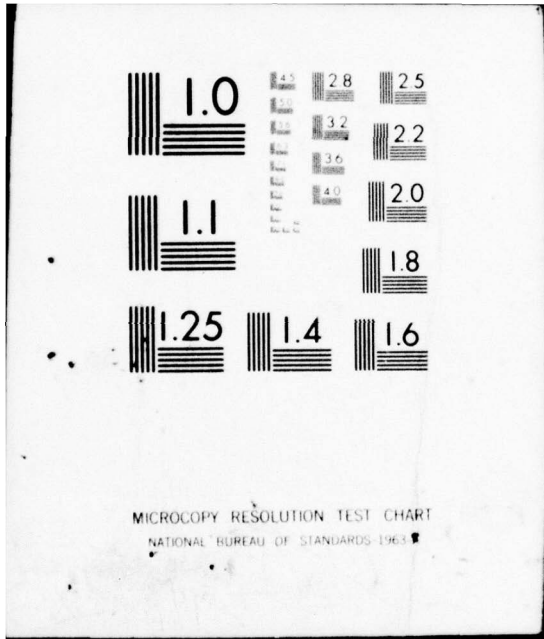
NL

1 OF 1  
AD  
A034007



END

DATE  
FILMED  
2-77



MICROCOPY RESOLUTION TEST CHART  
NATIONAL BUREAU OF STANDARDS-1963-A

ADAU34007

1



UNITED STATES AIR FORCE  
 AIR UNIVERSITY  
**AIR FORCE INSTITUTE OF TECHNOLOGY**  
 Wright-Patterson Air Force Base, Ohio

AFIT  
 1980-1981

AFIT  
 1980-1981

DDC  
 1980-1981

see 1473

ION IMPLANTATION  
IMPURITY ANALYSIS BY GLOW  
DISCHARGE OPTICAL SPECTROSCOPY

THESIS

GEP/PH/76-5

David S. Hake  
Capt USAF

ACCESSION for	
DTIC	White Section <input checked="" type="checkbox"/>
DOC	Buff Section <input type="checkbox"/>
UNANNOUNCED	<input type="checkbox"/>
JUSTIFICATION.....	
BY.....	
DISTRIBUTION/AVAILABILITY CODES	
Dist. AVAIL. and/or SPECIAL	
<b>A</b>	

Approved for public release: distribution unlimited

ION IMPLANTATION  
IMPURITY ANALYSIS BY GLOW  
DISCHARGE OPTICAL SPECTROSCOPY

THESIS

Presented to the Faculty of the School of Engineering  
of the Air Force Institute of Technology  
Air University  
in Partial Fulfillment of the  
Requirements for the Degree of  
Master of Science

by

David S. Hake, B.S.

Capt                      USAF

Graduate Engineering Physics

December 1976

Approved for public release; distribution unlimited.

Preface

I have attempted in this report to present the methodology and the results of an experimental study of measuring total impurity concentration profiles in unannealed ion-implanted gallium arsenide (GaAs) by use of the glow discharge optical spectroscopy (GDOS) technique. My efforts during the last three months involved the design, assembly and operation of a GDOS system at the Electronics Research Branch of the Avionics Laboratory (AFAL/DHR). This work has verified the applicability of the GDOS profiling technique for some group II p-type impurities implanted in GaAs. I hope that my efforts will have contributed to the development of a useful profiling technique for GaAs and will have laid the groundwork for further investigations of the GDOS technique applied to GaAs.

The bibliography included in this report is relatively complete and represents much of the current work which has been done using the GDOS technique.

Valuable guidance and assistance were provided to me by numerous people at the Avionics Laboratory, including Dr. Y. S. Park and SSgt. J. Ehret. I am particularly indebted to Captain Wayne Anderson of the same laboratory, who suggested this topic and who served as my laboratory research advisor. His valuable guidance, discussions, and encouragement were sincerely appreciated. Dr. Robert Hengehold, of the Air Force Institute of Technology Physics

Department served as the author's thesis advisor. I wish to express my sincere gratitude to these people for all their efforts in assisting me.

I appreciate the excellent glass work of J. Ray and P. Bell of the Avionics Laboratory and the excellent machine work provided by members of the AFIT machine shop. I also wish to thank my wife for her patience and aid in the preparation of this manuscript.

David S. Hake

## Contents

	Page
Preface . . . . .	ii
List of Figures and Tables . . . . .	vi
Abstract . . . . .	viii
I. Introduction . . . . .	1
II. Background . . . . .	4
Ion Implantation . . . . .	4
Energy Loss Mechanisms . . . . .	5
Range Statistics . . . . .	7
Glow Discharge . . . . .	10
Sputtering . . . . .	16
Glow Discharge Optical Spectroscopy (GDOS) . . . . .	18
III. Experimental Equipment . . . . .	22
The Discharge Chamber Assembly . . . . .	22
Discharge Chamber . . . . .	22
Argon Gas Source . . . . .	24
Electrical Equipment . . . . .	24
The Vacuum System . . . . .	25
GDOS Detection System . . . . .	25
Monochromator . . . . .	25
Photomultiplier Tube and Power Assembly . . . . .	26
Photomultiplier Housing Assembly . . . . .	26
Photon Counting Equipment . . . . .	26
Lock-In Amplifier System . . . . .	27
XY Recorder . . . . .	27
Sputtering Rate Measurement System . . . . .	28
Samples . . . . .	28
IV. Experimental Procedure . . . . .	29
Assembly and Testing of Equipment . . . . .	29
Vacuum Testing of the Discharge Chamber . . . . .	29
Production of the Discharge . . . . .	29
Optical System Alignment . . . . .	31
Operation of the GDOS System . . . . .	31
Determination of the Best Impurity Emission Lines . . . . .	34
Determination of Sputtering Rate and Sputtering Uniformity . . . . .	35
Sputtering Rate Studies . . . . .	35
Sputtering Uniformity . . . . .	37

## Contents

	Page
Calibration of the GDOS System . . . . .	38
Impurity Profiles . . . . .	39
V. Results and Discussion . . . . .	41
Investigation of the Discharge Spectrum . . . . .	41
Investigation of Sputtering Rate Parameters. . . . .	41
Effect of Voltage on Sputtering Rate. . . . .	45
Effect of Pressure on Sputtering Rate . . . . .	45
Correspondence Between Sputtering Rate and Emission Intensity . . . . .	47
Investigation of Sputtering Uniformity . . . . .	49
Investigation of GDOS Impurity Profiling . . . . .	54
Calibration of the GDOS System. . . . .	54
Impurity Profiles . . . . .	58
VI. Conclusions and Recommendations . . . . .	65
Conclusions . . . . .	65
Recommendations . . . . .	67
Bibliography . . . . .	70
Vita . . . . .	73

## List of Figures and Tables

<u>Figure</u>		<u>Page</u>
1	Definition of Range R and Projected Range $R_p$ . . .	8
2	Gaussian Distribution for Relative Light and Heavy Ions Implanted in an Amorphous Target . . .	9
3	(a) Regions of the Glow Discharge, (b) Light Intensity Distribution, (c) Voltage and Field Distribution. . . . .	11
4	Characteristics of the Normal and Abnormal Glow Discharge. . . . .	15
5	Sputtering and Excitation Process Near the Cathode . . . . .	20
6	Glow Discharge Chamber. . . . .	23
7	Schematic Diagram of the GDOS System. . . . .	30
8	Sample Mounted on the Cathode of the GDOS System.	32
9	Sputtered Step Heights Measured by the Dektak System . . . . .	36
10	Spectrum from Sputtered Cadmium (Solid Line) Superimposed on Spectrum of Undoped GaAs (Broken Line) . . . . .	42
11	Spectrum from Sputtered Zinc (Solid Line) Superimposed on Spectrum of Undoped GaAs (Broken Line) . . . . .	43
12	Spectrum from Sputtered Magnesium (Solid Line) Superimposed on Spectrum of Undoped GaAs (Broken Line) . . . . .	44
13	Sputtering Rate Versus Discharge Voltage. . . . .	46
14	Sputtering Rate Versus Discharge Pressure . . . . .	48
15	Intensity of Ga 4172.1 Å Emission Line Versus Discharge Voltage . . . . .	50
16	Intensity of Ga 4172.1 Å Emission Line Versus Sputtering Rate . . . . .	51

List of Figures and Tables

<u>Figure</u>		<u>Page</u>
17	Non-Uniform Lateral Sputtering of a GaAs Sample . .	52
18	Intensity of Ga 4172.1 Å Emission Line as Copper Film was Sputtered . . . . .	53
19	Intensity of Ga 4172.1 Å Emission Line During Initial Transient Period of the Discharge . . . . .	55
20	Spectrum from Sputtered $8 \times 10^{18}$ ions/cm <sup>3</sup> Zinc Doped GaAs (Solid Line) Superimposed on Spectrum of Undoped GaAs (Broken Line) . . . . .	56
21	Spectrum from Sputtered Zinc (Solid Line) Superimposed on Spectrum of Undoped GaAs (Broken Line) . .	57
22	Effects of Sputtering Si <sub>3</sub> N <sub>4</sub> Cap (Solid Line) on GaAs Versus Uncapped GaAs (Broken Line) While Monitoring the Cd 3610.5 Å Emission Line . . . . .	60
23	Relative GDOS Measured Profile of Zinc Implanted GaAs Compared to Theoretical ISS Profile . . . . .	61
24	Relative GDOS Measured Profile of Magnesium Implanted GaAs Compared to Theoretical ISS Profile. .	62
25	Relative GDOS Measured Profile of Gallium Implanted Silicon Compared to Theoretical ISS Profile . . . . .	64

<u>Table</u>		<u>Page</u>
I.	Data-Sputtering Rate Versus Voltage	45
II.	Data-Sputtering Rate Versus Gas Pressure	47
III.	Data-Emission Intensity Versus Voltage	49

Abstract

The Glow Discharge Optical Spectroscopy (GDOS) technique was investigated to determine if it could be used to measure total impurity concentration profiles in unannealed ion implanted GaAs. Cadmium, zinc, and magnesium ions, which are common p-type dopants in GaAs, were implanted at energies of 99 keV and 120 keV and fluences ranging from  $10^{14}$  to  $10^{16}$  ions/cm<sup>-2</sup>. The implanted GaAs samples were sputtered in a low pressure dc glow discharge using argon gas. Intensity of a strong emission line, characteristic of the implanted impurity, was monitored as a function of time. This intensity was combined with independently measured GaAs substrate sputtering rates to calculate total impurity concentration profiles. Uncalibrated concentration profiles were obtained for Zn and Mg in GaAs. None was obtained for Cd.

ION IMPLANTATION  
IMPURITY ANALYSIS BY GLOW  
DISCHARGE OPTICAL SPECTROSCOPY

I. Introduction

The Air Force is interested in developing semiconductor devices having higher electron mobilities and band gaps than present devices made of silicon or germanium. Gallium arsenide (GaAs), a semiconducting compound consisting of group III and group V elements of the periodic table, satisfies these requirements for device applications. The Electronics Research Branch of the Avionics Laboratory (AFAL/DHR) is developing the basic technology needed to produce devices using GaAs substrate.

Ion implantation is a relatively new technique used for doping semiconductor substrates with impurity ions. It is a very useful doping technique because it can be used to implant almost any impurity ion into almost any semiconductor material. Conventional diffusion doping methods are very limited in this respect.

In ion implantation, the desired impurity ions are implanted by accelerating them in an ion accelerator and then bombarding the semiconductor substrate with the ion beam. Precise control of the ion beam allows the production of devices having precise and tailor-made ion distribution profiles which leads to more efficient devices.

In order to perfect the technology necessary to produce GaAs devices, it is necessary to develop a fast, accurate, and relatively inexpensive method for measuring the total impurity concentration profile implanted in the GaAs substrate before annealing.

Several methods are currently used to do this, mainly Secondary Ion Mass Spectroscopy (SIMS) and Auger measurements. SIMS provides excellent depth resolution to about 10 Å, but requires expensive and complex equipment (Ref 17: 385-391). The Auger method is also expensive. Another method which can be used is the Radio-Tracer method which is accurate but suffers from the fact that radioactive isotopes of the impurity ion of interest must be implanted and for many impurities there are no radioactive isotopes.

The purpose of this investigation was to evaluate the glow discharge optical spectroscopy (GDOS) technique as a method of measuring the total impurity profile in an ion implanted GaAs substrate before annealing.

In GDOS, the target substrate is dc sputtered in argon and the glow discharge is monitored for luminescence corresponding to a particular implanted impurity. The luminescence intensity combined with the known substrate sputtering rate provides an estimate of the impurity concentration profile in the substrate.

The remainder of this report is devoted to a background discussion of ion-implantation, the glow discharge, and the

GDOS method, followed by a description of the experimental equipment and procedure used in this investigation. The results obtained from this study are then presented and analyzed in relation to theory and other findings. The final chapter of this report contains conclusions drawn from the study and recommendations for future study of the GDOS technique.

## II. Background

### Ion Implantation

Ion implantation is the process of bombarding a substrate with energetic ions of uniform mass and energy which produces a spatial distribution or profile of the incident ions below the substrate surface.

Historically, the first attempt at ion implantation for the purpose of producing a semiconductor device was made in 1955 by Cussins, who implanted boron ions into a germanium substrate (Ref 8:296). Theories necessary for predicting the implanted ion distribution in amorphous targets have been developed since that time.

The most widely accepted is the Lindhard, Scharff, and Schiott (LSS) range distribution theory developed in 1963 (Ref 18:1-39). This theory assumes ion implantation into an amorphous target or purposely misaligned crystalline target, and that sputtering of surface atoms is negligible. Quantum effects are neglected when treating energy losses to electrons in the target.

Gallium Arsenide has a zinc-blende structure of two inter-penetrating fcc sub-lattices. The (111) face is composed of Ga atoms and the  $\bar{1}\bar{1}\bar{1}$  face is composed of As atoms (Ref 6:262). For the purpose of this investigation, the GaAs samples were cleaved along the (100) direction but purposely misaligned approximately  $7^\circ$  from the normal for

implantation. Thus the GaAs targets were effectively amorphous and the LSS theory should be applicable. The 99 to 120 keV implant energies used in this study were low enough to assume negligible surface sputtering due to implantation.

Energy Loss Mechanisms. In the LSS theory, the total distance or range that an ion travels into a target is calculated by considering the energy losses it experiences due to collisions with target nuclei and electrons as it penetrates into the target. These two energy loss mechanisms are assumed to be independent of one another and the average rate of energy loss per path length for an incident ion as it penetrates the target is given by

$$-\frac{dE}{dx} = N \left( S_n(E) + S_e(E) \right) \quad (1)$$

where  $E$  is the energy of the incident ion at a distance  $x$  into the target,  $S_n(E)$  is the nuclear stopping power,  $S_e(E)$  is the electronic stopping power, and  $N$  is the average number of target atoms per unit volume (Ref 8:298).

In a first approximation, the nuclear stopping power,  $S_n(E)$  is independent of the incident ion energy and depends only on the atomic numbers and masses of the interacting particles. Nuclear stopping is assumed to be a two body elastic scattering process, independent of other target nuclei. This is based on small angle scattering and is a

good approximation for amorphous and misaligned single crystal targets (Ref 21:11). Nuclear stopping predominates for heavy ion and low implant energies, such as the zinc and cadmium ions used in this study. The nuclear stopping power is given by

$$S_n = 2.8 \times 10^{-15} \frac{Z_1 Z_2}{(Z)^{1/3}} \frac{M_1}{M_1 + M_2} \text{ eV} \cdot \text{cm}^2 \quad (2)$$

where

$$Z^{1/3} = \left( Z_1^{2/3} + Z_2^{2/3} \right)^{1/2} \quad (3)$$

and where  $Z_1$  and  $M_1$  are the atomic number and mass of the incident ion while  $Z_2$  and  $M_2$  are those of the target (Ref 8:298-299).

Electronic stopping power is more difficult to calculate than nuclear stopping power. In the ISS model, the electrons in the target are visualized as being a free electron or Fermi gas. The electronic stopping power is given by

$$S_e(E) = cv = kE^{1/2} \quad (4)$$

where  $v$  is the velocity and  $E$  is the energy of the implanted ion,  $c$  and  $k$  are constants which depend on the target material and are approximately independent of incident ion species for amorphous targets (Ref 8:303). Electronic stopping power predominates for high implant energies and

light ions, such as the magnesium ions used in this investigation.

Range Statistics. Once the stopping powers are known, the average total distance or range  $R$ , that the incident ion penetrates into the target substrate can be found by integrating equation (1) and is given by

$$R = \int_0^R dx = \frac{1}{N} \int_0^{E_0} dE / [S_n(E) + S_e(E)] \quad (5)$$

where  $N$  is the number of target atoms per unit volume,  $E$  is the energy of the ion at some distance  $x$  from the target surface while  $S_n(E)$  and  $S_e(E)$  are the nuclear and electronic stopping powers respectively (Ref 8:299). The projection of this range on the incident ion direction is called the projected range  $R_p$ , which is measured experimentally. The concept of range and projected range is shown in Figure 1.

Due to the randomness of collisions between incident ions and target atoms, incident ions having the same mass and energy come to rest in the substrate at different depths forming a range distribution. It is approximately Gaussian in amorphous targets and is shown in Figure 2 for cases where the ion mass is greater than and less than the mass of the target atoms (Ref 21:3). The Range  $R$  and projected range  $R_p$  are distribution functions characterized by mean values  $\bar{R}$  and  $\bar{R}_p$  and their standard deviations,  $\Delta\bar{R}$  and  $\Delta\bar{R}_p$ . These qualities are tabulated for the ions and substrate

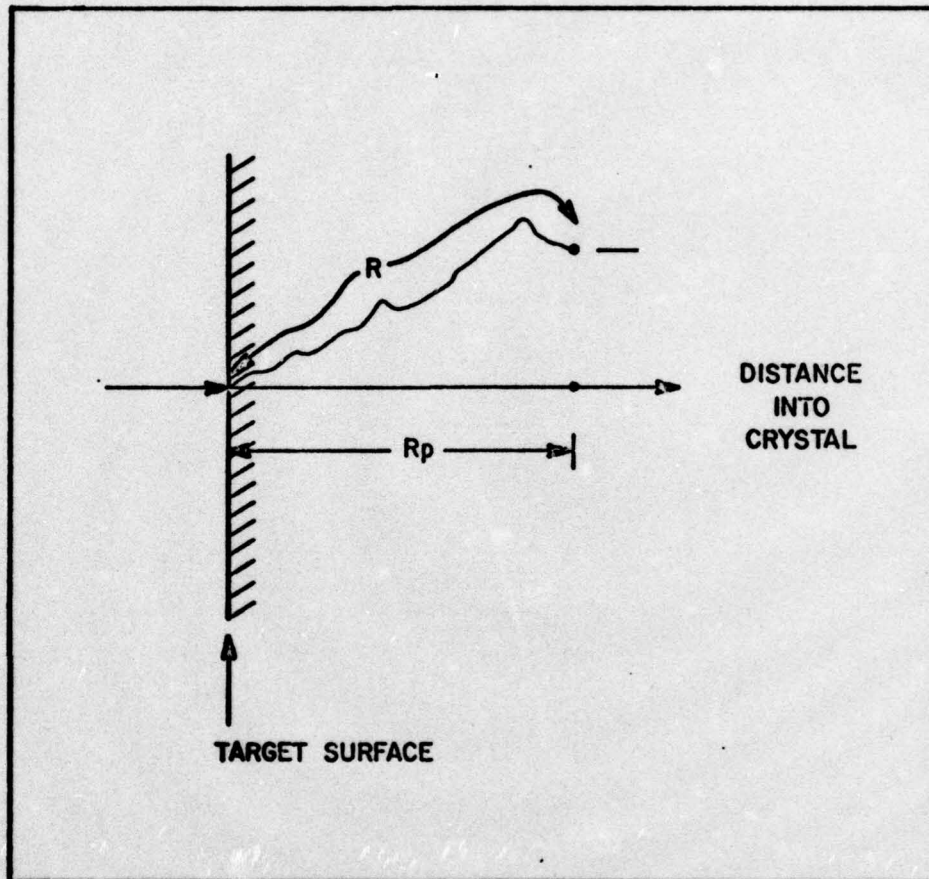


Figure 1. Definition of Range R and Projected Range R<sub>p</sub> (From Ref 8:298)

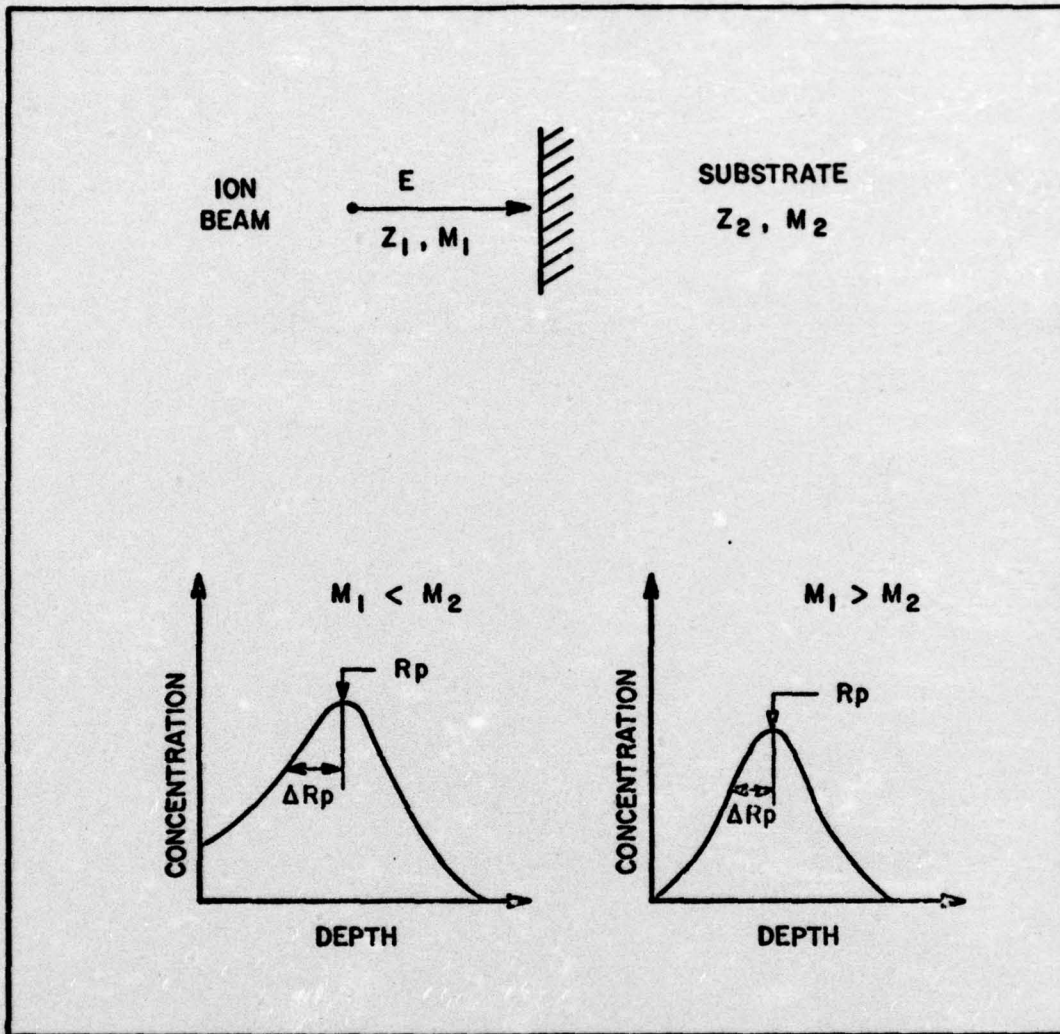


Figure 2. Gaussian Distributions for Relative Light and Heavy Ions Implanted in an Amorphous Target (From Ref 21:3)

materials used in this investigation (Ref 9). Tabulations for Mg ions in GaAs were not available, so calculations for Al in Germanium were used as the masses of the ions and substrates closely matched.

The Gaussian concentration distribution of ions in the substrate is given by

$$N(x) = N_p \exp \left[ -(x-R_p)^2 / 2 \Delta R_p^2 \right] \quad (6)$$

where

$$N_p = \phi / \left[ \sqrt{2\pi} \Delta R_p \right] \quad (7)$$

$N(x)$  is the ion concentration at a depth  $x$  below the target surface,  $N_p$  is the peak concentration at the depth  $R_p$ , and  $\phi$  is the ion implant fluence in ions/cm<sup>-2</sup> (Ref 9:22).

### Glow Discharge

When the pressure in a discharge tube is less than 0.1 mm of Hg and a voltage is applied across the electrodes, a glow discharge characterized by alternately light and dark regions is produced between the electrodes as shown in Figure 3 (Ref 1:213). Also shown in the figure are the variations in light intensity voltage and electric field associated with each region of the discharge.

The nature of the discharge depends on the gas, pressure, size, material, and separation of the electrodes.

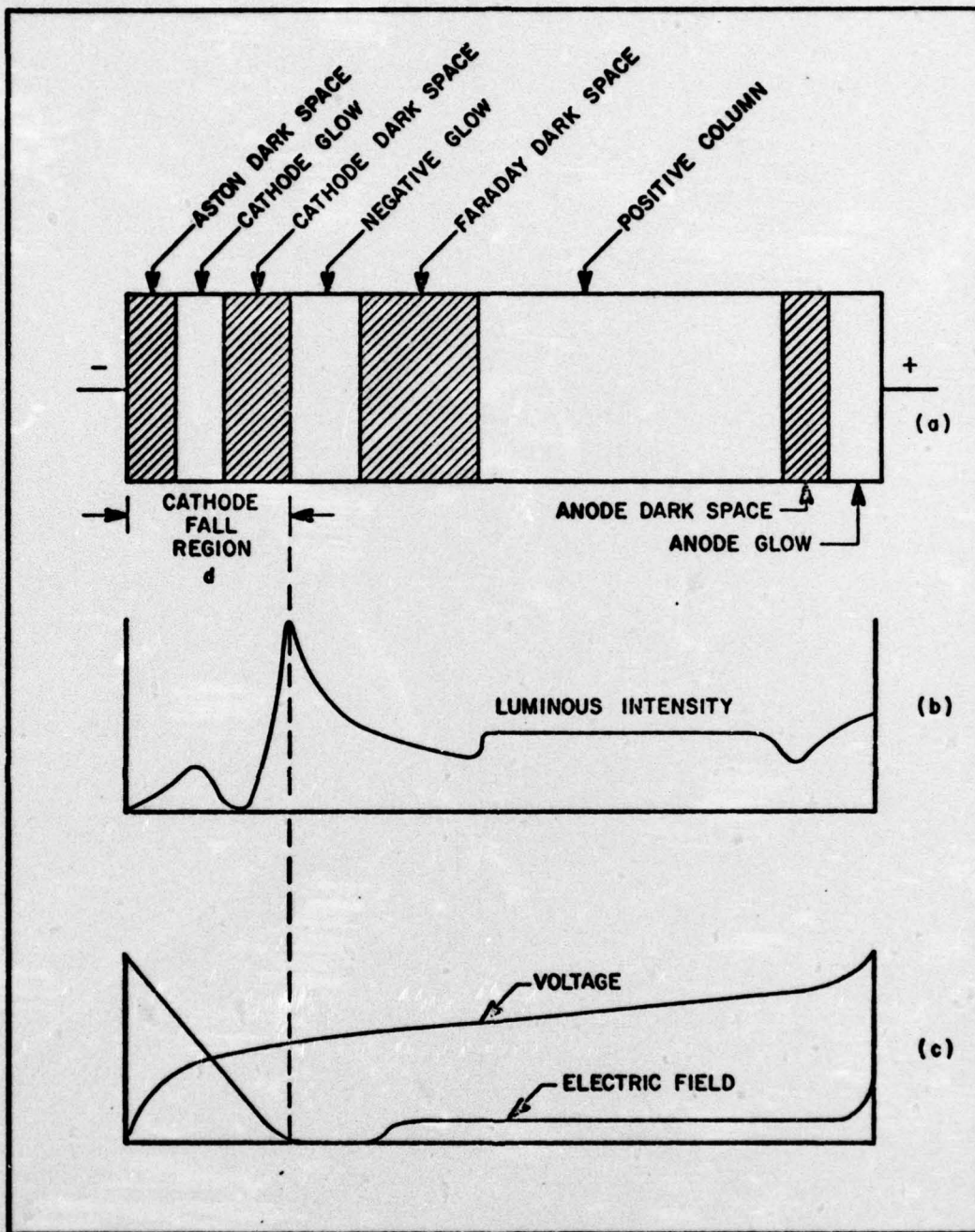


Figure 3. (a) Regions of the Glow Discharge, (b) Light Intensity Distribution, (c) Voltage and Field Distributions (From Ref 1:213)

For Argon, the discharge is blue (Ref 19:565). Decreasing gas pressure increases the size of the negative glow and Faraday dark space regions, while it causes the positive column to decrease or disappear. Decreasing the electrode separation causes a decrease in positive column length, but does not affect the size of the other regions.

The discharge is produced when gas molecules are ionized and the resulting positive ions are attracted and accelerated toward the cathode. These ions strike the cathode surface and are neutralized. Electrons are emitted if the energy of the incident ion is at least twice as great as the work function of the cathode material (Ref 19:576). The number of electrons emitted per incident gas ion is called the secondary electron emission coefficient (Ref 7:220). The electrons emitted from the cathode are accelerated toward the anode. The luminous regions of the discharge are a direct result of this movement.

The electrons emitted from the cathode initially have energies too low to collisionally excite gas molecules even though the electric field is large near the cathode. This then accounts for the dark region next to the cathode called Astons dark space. Outside this region the electrons have acquired sufficient energy through acceleration to correspond to maximum collisional excitation of the gas molecules. The gas molecules are excited and light is emitted upon deexcitation. This luminous region is called the cathode glow region.

Emitted cathode electrons which have accelerated beyond this point without experiencing any collisions have enough energy to ionize the gas, which for argon is 15.755 eV (Ref 13:E-68). Electrons emitted due to this ionization are accelerated toward the anode, but have too little energy to excite the gas molecules, and this results in the region called the cathode dark space.

These electrons from the cathode dark space are accelerated by the electric field and eventually attain sufficient energy to collisionally excite gas molecules, again causing emitted light. This region is called the negative glow region. The emitted light is less intense than in the cathode glow region.

Having lost their energy through collisions in the negative glow region, the electrons again lack energy sufficient to excite or ionize the gas, but are accelerated toward the anode in a weak electric field. This results in the region called the Faraday dark space.

The electrons leaving this region enter a region which has a small, almost constant electric field, and where there is approximately charge neutrality. The electrons are slow in this region, but have relatively high momentum compared to that of the positive gas ions since the electron temperature is several tens of thousands of degrees, while the gas ions are approximately at ambient temperature (Ref 22:132). This region is called the positive column and light emitted from it is next in brightness to the cathode glow.

This investigation utilizes the abnormal glow discharge which will be described here in relation to what is called the normal glow discharge.

The normal glow discharge is produced when the discharge is operating at low currents. The cathode is only partially covered by the cathode glow. Increasing the current only increases the amount of cathode covered. The current density  $j_c$  at the cathode is constant, independent of the discharge current  $i_c$  and the cathode fall potential  $V$ . These effects are shown in Figure 4 (Ref 1:214).

Once the current is increased beyond a critical value, the current density  $j_c$  and the cathode fall potential  $V$  at the cathode are no longer constant, but begin to increase with increasing current as shown in Figure 4. When this happens the cathode is completely covered by the glow, and this is known as the abnormal glow discharge. In the abnormal glow discharge, the cathode fall potential and the thickness of the cathode fall region  $d$  are given respectively by

$$V = E + \frac{F \sqrt{j}}{p} \quad (8)$$

and

$$d = \frac{A}{p} + \frac{B}{\sqrt{j}} \quad (9)$$

where  $j$  is the current density,  $p$  is the pressure, and  $A$ ,  $B$ ,  $E$ , and  $F$  are constants for a particular gas and cathode

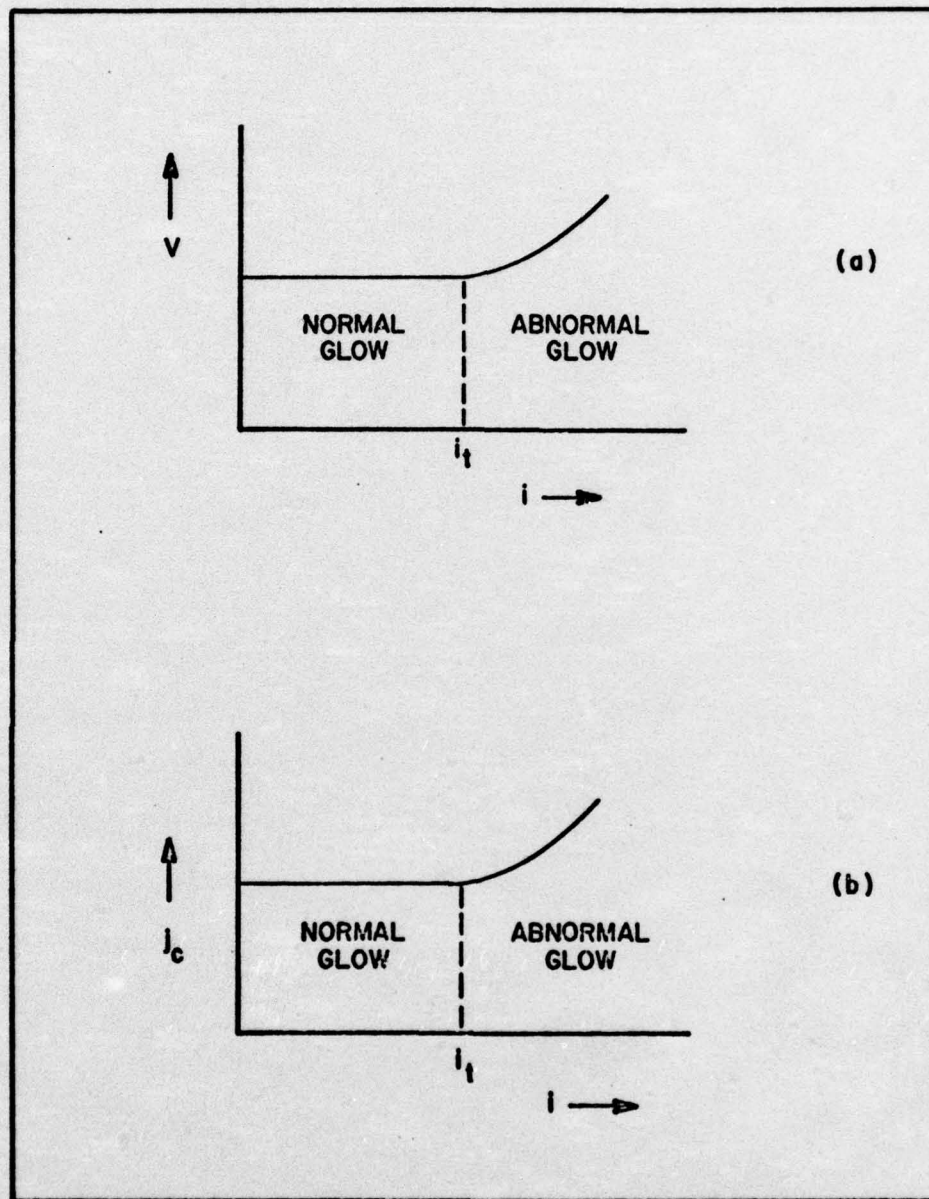


Figure 4. Characteristics of the Normal and Abnormal Glow Discharge (From Ref 1:214)

material. Eliminating the current density between these equations gives

$$pd = A + \frac{BF}{V-E} \quad (10)$$

which relates the gas pressure, thickness of the cathode fall region, and the cathode fall potential in the abnormal glow discharge (Ref 1:226-227).

### Sputtering

Sputtering is the process in which material is continually removed from a surface either by reactive or physical processes.

In this investigation, physical sputtering resulting from the abnormal glow discharge is used. Incident positive ions bombard the cathode surface and sputter off neutral material. Sputtering of the surface due to chemical reactions is neglected because the cathode is sputtered in a low pressure inert gas, which minimizes chemical reactions leading to reactive sputtering.

Current sputtering theories involve collision models involving momentum transfer. Sputtering results when energetic positive gas ions penetrate the target surface and collide with target atoms. The resulting momentum transfer in the elastic collisions is transferred back toward the target surface and if the momentum transfer is large enough to overcome surface binding energy, neutral surface atoms are ejected (Ref 15:221-237). In crystals

such as GaAs, the momentum is transferred along crystallographic or close packing directions resulting in preferential sputtering in certain directions (Ref 25:1821). Studies using GaAs involving normally incident bombardment of 100 to 600 eV argon ions in an argon glow discharge indicate that the sputtering yield is slightly higher for the (111) face than for the ( $\bar{1}\bar{1}\bar{1}$ ) or (110) faces (Ref 2:5738 and Ref 4:5184).

Sputtering yield is normally defined as the total number of ejected atoms per incident ion. In the glow discharge, the sputtering yield is proportional to the voltage and current, and is inversely proportional to the pressure and distance between electrodes (Ref 1:229-230). Sputtering yield is lowered for higher pressures since incident positive ions experience more collisions while moving toward the cathode and therefore strike the cathode with less energy. Sputtering at higher pressures also may cause increased contamination of the discharge since ejected atoms will lose energy quickly due to increased collisions and are likely to fall back into the cathode.

Sputtering yield also depends on the target material (Ref 1:229-230). Studies show that the sputtering yield is greater for GaAs than for silicon under identical conditions in an argon glow discharge (Ref 24:6). Additionally, sputtering yield is a function of the mass, energy, and angle of incidence of the positive ions. The yield is a maximum near normal incidence and increases for

higher ion mass and energy (Ref 28:679). Studies indicate that sputtering yield is fairly insensitive to target temperatures even at 400° to 1000°C (Ref 15:163).

The material sputtered from the surface of the cathode in the glow discharge consists almost entirely of neutral atoms. A mass-spectroscopic study of sputtering from single crystals of GaAs by low energy argon ions was conducted by J. Comas and C. B. Cooper. They analyzed the sputtered material from the (110), (111), and ( $\bar{1}\bar{1}\bar{1}$ ) faces of GaAs (Ref 3:2956-2960). It was found that approximately 99.4 per cent of the collected material was neutral Ga and As atoms and the remaining 0.6 per cent were neutral GaAs molecules. Approximately equal amounts of Ga and As were found.

#### Glow Discharge Optical Spectroscopy (GDOS)

Glow discharge optical spectroscopy refers to the study of the emission spectra resulting from dc cathode sputtering in a low pressure gas discharge operated in the abnormal glow mode. Historically, von Hippel first reported observing emission spectra resulting from sputtered atoms in a glow discharge (Ref 14:672). Stuart and Wehner later measured sputtering yields using the emission intensity from a dc glow discharge and showed that the intensity of a spectral line of the target material was proportional to the density of the target atoms in the region of the discharge under observation, assuming the density of target

atoms was proportional to the sputtering yield (Ref 26:2345-2347). Green and Whelan first proposed the use of emission spectroscopy as a technique for detecting trace elements and measuring impurity profiles in thin films (Ref 12:2509).

In the GDOS technique, neutral atoms are dc sputtered in a low pressure abnormal glow discharge between two electrodes. The sputtered neutral atoms are collisionally excited by electronic collisions in the glow discharge as shown in Figure 5 (Ref 20:15). The atoms become de-excited and emit characteristic luminescence which is monitored by a monochromator.

The GDOS technique can be used to measure the chemical composition of a material by independently measuring the sputtering rate of the material and the intensity of the emission spectral line which has been calibrated using known standards.

It was in this context that the GDOS technique was applied to ion implanted GaAs in this investigation. By independently measuring the sputtering rate of GaAs and the intensity of a strong characteristic spectral line of the implanted impurity, the profile of the impurity could be measured.

There are several assumptions which enter into this technique. First, the chemical composition of material sputtered into the glow discharge plasma is representative of that of the solid. This requires that the target substrate must be uniformly sputtered for accurate profiling

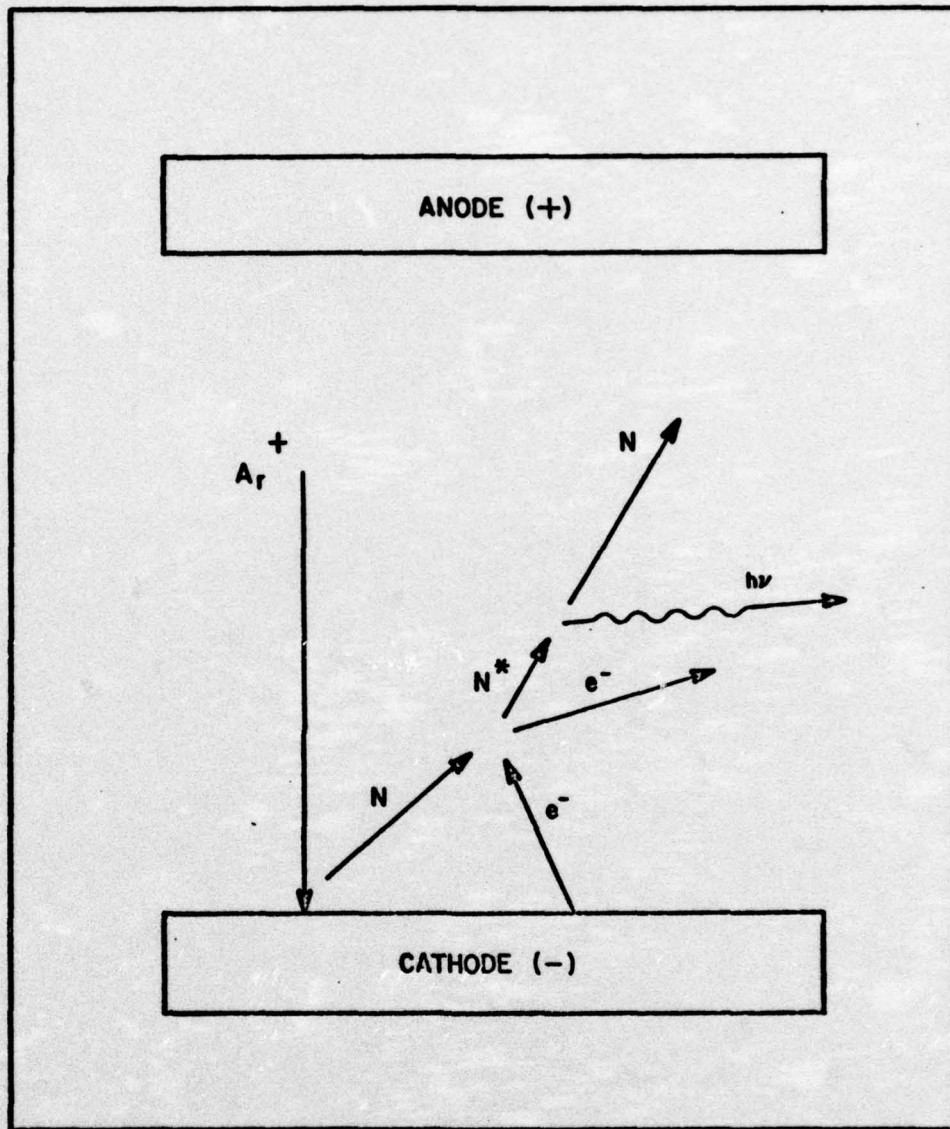


Figure 5. Sputtering and Excitation Process Near the Cathode (From Ref 20:15)

to work. A second requirement is that the excitation probability of sputtered atoms in the plasma is independent of concentration of the various species in the plasma, which means that emission intensity is assumed to be proportional to the concentration of a sputtered species in the plasma (Ref 11:2701). For the GDOS technique to be accurate, the sputtering rate should be uniform and the sputtered atoms should be ejected from the discharge, so as not to contaminate the discharge.

The GDOS technique has been shown to be effective in analytical depth profiling for ion implanted boron in silicon (Ref 10:366-369). Additionally, it has recently been used to estimate concentration profiles in thin films grown on GaAs (Ref 12:2509-2513).

Chapter II of this report describes the experimental equipment used in this investigation.

### III. Experimental Equipment

This chapter is devoted to the detailed description of the experimental equipment used in this investigation. The equipment is classified into the following systems for description:

1. The discharge chamber assembly.
2. The vacuum system.
3. The GDOS detection system.
4. Sputter rate measurement system.
5. Samples.

#### The Discharge Chamber Assembly

The glow discharge chamber assembly equipment includes the discharge chamber, argon gas source, and electrical equipment.

Discharge Chamber. The particular discharge chamber used in this investigation was obtained from the Avionics Laboratory and modified for this experiment. A diagram of the chamber is presented in Figure 6. The chamber was made from an 8-3/4 inch diameter, 7 inch high pyrex glass cylinder with 1/4 inch thick walls. A 2 inch diameter 1/8 inch thick quartz window was installed on the side of the chamber for ultraviolet light transmission. The top and bottom parts of the discharge chamber were made of 1/2 inch thick, 10 inch diameter stainless steel plates. The top plate formed the anode assembly while the bottom plate formed the cathode

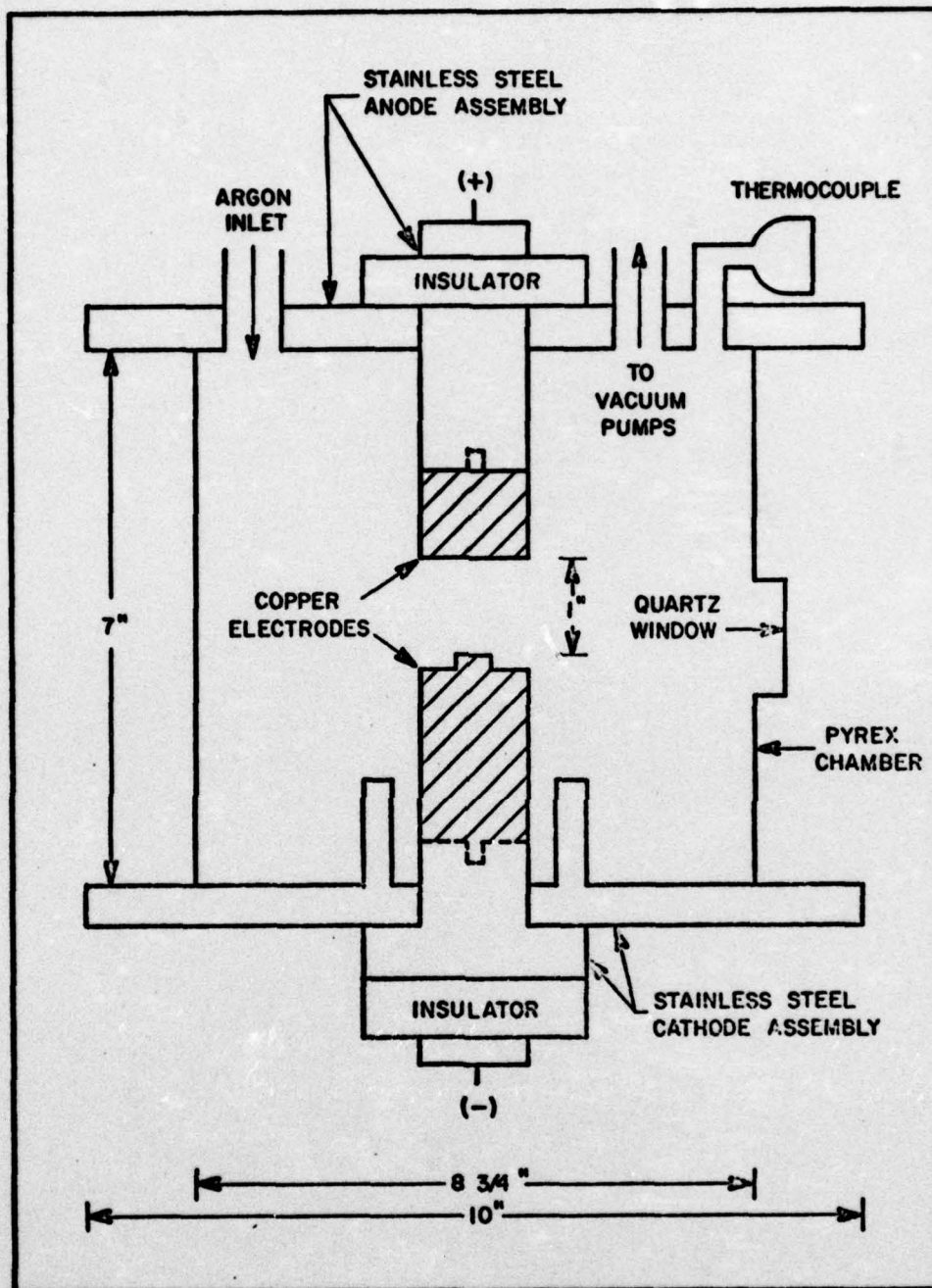


Figure 6. Glow Discharge Chamber

assembly. A gas inlet port, a vacuum port, and a thermocouple gauge were mounted on the anode assembly. Rubber rings provided a vacuum seal between the anode and cathode plates and glass chamber. The discharge chamber was mounted on an aluminum tripod stand which was designed for the experiment.

The cylindrical electrodes were made from one inch diameter solid copper. The lengths of the anode and cathode were 1 inch and 1-7/8 inches respectively. Electrode separation was one inch. The cathode has a 3/16 inch diameter, 1/16 inch high cylindrical stub protruding from the top on which samples were mounted.

Argon Gas Source. Argon gas was supplied to the chamber from a standard high pressure regulator. Gas purity was approximately 99.9 per cent. Constant gas flow to the discharge chamber was controlled by an Andonian Cyrogenics, Inc. leak valve.

Electrical Equipment. A potential difference was produced between the electrodes in the discharge chamber by use of a Keithly Instruments Model 242 D.C. Regulated High Voltage Power Supply which supplied 300 to 3500 volts at 0 to 25 milliamps. The anode was kept at ground potential and negative voltage was impressed on the cathode. Current in the discharge was measured using an ammeter in the cathode circuit. A 312 Kohm load resistance was used between the power supply and the cathode to reduce heating in the discharge and prevent arcing as the discharge was started.

### The Vacuum System

A Varian/Vacuum Division Model PS-10 Pumping Station was used to evacuate the discharge chamber. The PS-10 is a standard pumping station equipped with a mechanical fore-pump, a high vacuum diffusion pump, and associated valves and thermocouples. The diffusion pump provided vacuum to below one micron of mercury. Vacuum pressure in the discharge chamber was measured using a Consolidated Vacuum Corporation Model GIC-110 Ionization Vacuum Gauge connected to a thermocouple mounted on the anode assembly.

### GDOS Detection System

The GDOS detection system is based on a technique proposed by Green and Whelan (Ref 12:2509) previously described in Chapter II. A monochromator is used to monitor emission lines characteristic of atoms sputtered in a dc glow discharge. Intensity of the lines is measured using a photomultiplier tube whose output is measured by either a photon counting or lock-in amplifier system and then recorded.

Monochromator. A Spex Industries, Inc. Model 1704 1-meter Czerny-Turner Scanning Monochromator was used in this investigation for locating impurity emission lines and for monitoring the intensity of an impurity emission line as a function of time in the profiling experiments. The monochromator provided scan speeds from 1 to 1000 Angstroms per minute and a wavelength scale accurate to within 0.1 Å. The grating used had a 128 x 102 mm ruled area with 1200 lines/mm and was blazed at 5000 Å.

Photomultiplier Tube and Power Supply. An RCA C31034A 11-stage Quantacon photomultiplier tube and ultraviolet-transmitting glass window was used in the investigation. The tube had a typical amplification of  $3 \times 10^5$  and was highly suitable for photon counting when cooled. The typical dark count when cooled was below 15 counts per second and typical dark current was  $10^{-11}$  amp. D.C. power was supplied to the photomultiplier tube cathode by a Fluke Model 412B D.C. High Voltage Power Supply with an output range of 0 to 2.1 K volt.

Photomultiplier Housing Assembly. A Products for Research, Inc. Model TE-104 thermoelectrically refrigerated chamber was used to cool the photomultiplier tube. It was capable of cooling the tube to below  $-20^{\circ}$  C at up to  $+50^{\circ}$  C ambient temperatures, with the only external cooling equipment being a source of flowing water to dissipate heat from the housing's heat exchanger. The housing had an evacuated cylindrical chamber, with a converging lens on one end, which transmitted light to the photocathode while keeping moisture from the housing interior. The chamber which was supplied with the housing, would not transmit the ultraviolet light, so another chamber was devised for the experiment. It had quartz windows for ultraviolet light transmission, but lacked a focusing lens, which resulted in a 50 per cent signal reduction to the photomultiplier.

Photon Counting Equipment. A Model 1108 Multi-Mode Processor and Model 1120 Amplifier/Discriminator, both manufactured by SSR Instruments Co., a subsidiary of Princeton

Applied Research Corp., were used for photon counting, which was the primary luminescence detection system used in this investigation. The 1108 multi-mode processor is a high speed counter/timer which could be preset for count times from 1 microsecond to 999 seconds or total counts up to a  $10^8$  count capacity. The system had a pulse pair resolution of 12 nanoseconds and a maximum count rate of 85 MHz. The normal mode of operation in this study was counting for a preset time of from 0.1 to 2 seconds.

Lock-In Amplifier System. For part of this investigation, a standard lock-in amplifier system was used to detect emitted luminescence. A Princeton Applied Research Corporation (PAR) Model 191 variable speed chopper with a chopping frequency range of 15 to 600 Hz was used to chop light to the monochromator. PAR Model 221 and Model 116 pre-amplifiers and a PAR Model 124A Lock-In Amplifier were used to amplify and measure signals from the photomultiplier tube through a load resistance of 1 megohm. The lock-in amplifier was capable of accurate signal measurements from about 100 picovolts up to 500 millivolts at frequencies from 0.2 Hz to 210 KHz.

XY Recorder. Signal output from either luminescence detection system were displayed on the Y-axis of a Honeywell 500 XY Recorder. The X-axis presented elapsed time. X-axis scan speeds ranged from 0.2 to 10 inch/sec while the Y-axis sensitivities ranged from 1 millivolt to 100 volts/inch.

### Sputter Rate Measurement System

A Sloan Dektak Surface Measuring System consisting of the Dektak and associated chart recorder was used to measure sputtered steps in all samples. The Dektak employed a sensing head with a diamond stylus tracking at a constant preset tracking force to measure surface step heights from 25 to 1,000,000 Å.

### Samples

All samples used in this investigation were implanted at the Avionics Laboratory using an accelerator manufactured by Accelerators, Inc., Austin, Texas. It had a maximum implant potential of 150 keV. All samples were mounted at approximately  $7^\circ$  from the normal to the beam to avoid channeling effects and were implanted at room temperature. The samples were melt-grown, undoped GaAs crystals, cleaved and polished along the (100) face. Most samples used were approximately 5 mm x 3 mm x 0.2 mm. All had resistivities of 0.0350 to 0.0520 ohm-cm. Cadmium and zinc ions were implanted at energies of 120 to 135 keV and fluences of  $10^{14}$ ,  $10^{15}$ , and  $10^{16}$  ions/cm<sup>2</sup>. Magnesium ions were implanted at 99 keV at fluences of  $10^{15}$  and  $5 \times 10^{15}$  ions/cm<sup>2</sup>. Some gallium ions were implanted at 120 keV into silicon at a fluence of  $10^{15}$  ions/cm<sup>2</sup>.

The experimental procedures used in this investigation are presented in Chapter IV.

#### IV. Experimental Procedure

The purpose of this study, as stated in the introduction, was to investigate the application of the GDOS technique to total impurity profiling in ion implanted GaAs. The experimental work was therefore directed toward the following areas:

1. Assembly and testing of equipment.
2. Operation of the GDOS system.
3. Determination of the best impurity emission lines.
4. Determination of sputtering rate and sputtering uniformity.
5. Calibration of the GDOS system.
6. Impurity profile measurements.

##### Assembly and Testing of Equipment

The initial part of this study involved the design, construction, and assembly of the equipment described in Chapter III and shown schematically in Figure 7 of this chapter.

Vacuum Testing of the Discharge Chamber. The discharge chamber was tested for leakage. Once leaks were sealed, the chamber could be evacuated to below ten microns of Hg within 30 minutes and below one micron of Hg within two hours.

Production of the Discharge. Production of the discharge was tested by applying up to 3000 volts to the electrodes. Arcing produced fluctuating discharge current and intensity. Discharge stability was achieved by placing

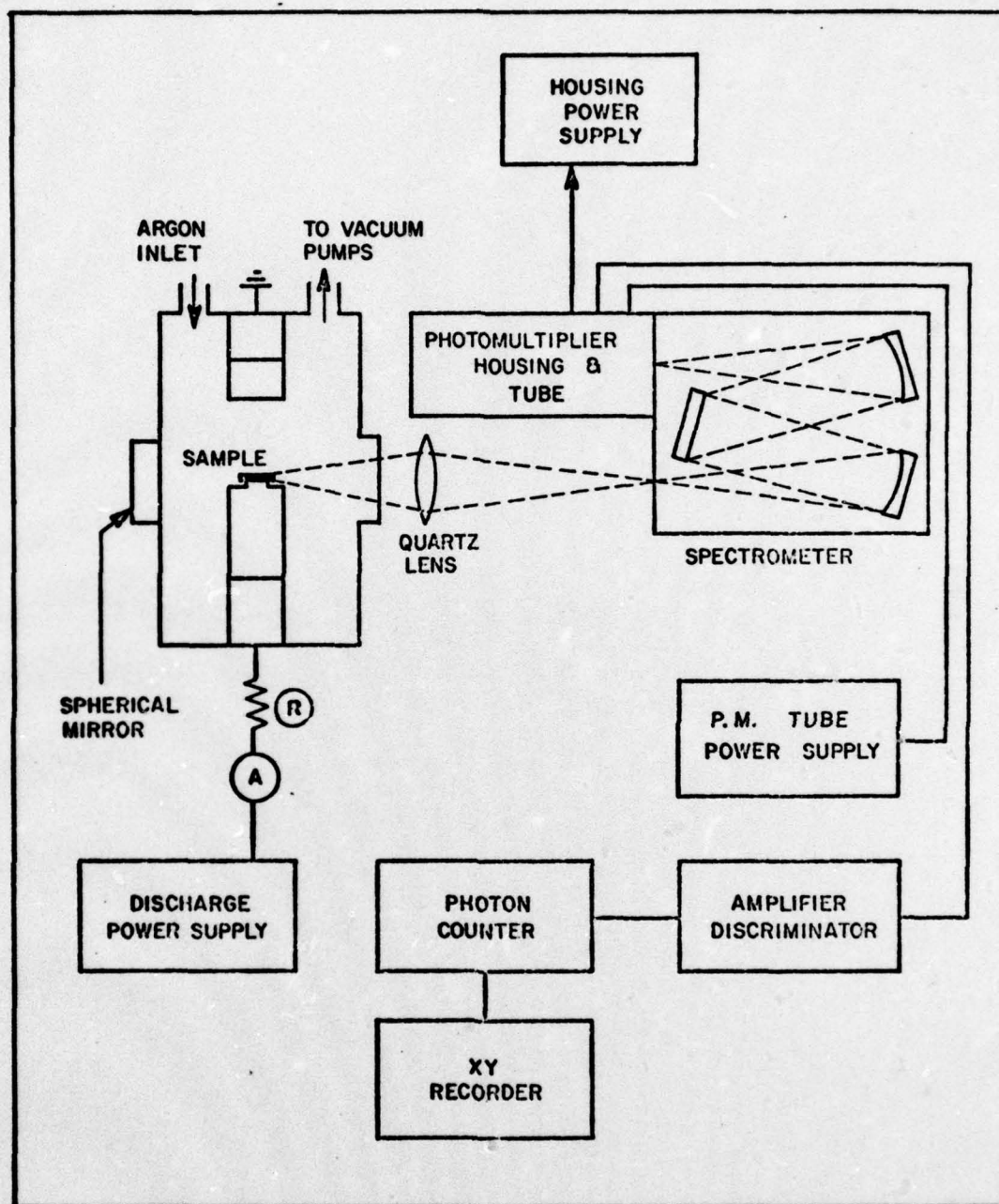


Figure 7. Schematic Diagram of the GDOS System

a 312 Kohm load resistance in the power supply circuit, eliminating sharp corners on the electrodes, and covering all but the ends of the electrodes by glass or quartz shields. The discharge was then stable for up to 3000 volts at pressures from 30 to over 100 microns.

Optical System Alignment. The cathode/target area, quartz lens, and monochromator entrance slit were adjusted so as to lie in the same horizontal plane. Alignment was checked using a small Spectra Physics He-Ne laser. An attempt was made to match the f-number of the lens and monochromator. Hg, Ne, and Ar calibration lamps, were used to calibrate the monochromator from 2000 Å to 7000 Å.

#### Operation of the GDOS System

The sample to be sputtered was mounted on the cathode as shown in Figure 8. Access was gained to the cathode by simply removing the anode assembly from the top of the chamber. The sample was placed on the cathode. The remainder of the cathode was shielded from sputtering by use of the quartz shield. The quartz shield minimized emission spectra in the discharge resulting from cathode sputtering.

The discharge chamber was evacuated below ten microns of Hg using the PS-10 pumping station diffusion pump with the argon source closed. This helped to remove gas impurities in the chamber which could contaminate the sample surface. The chamber was then backfilled with high purity argon gas and a constant flow of gas was maintained during

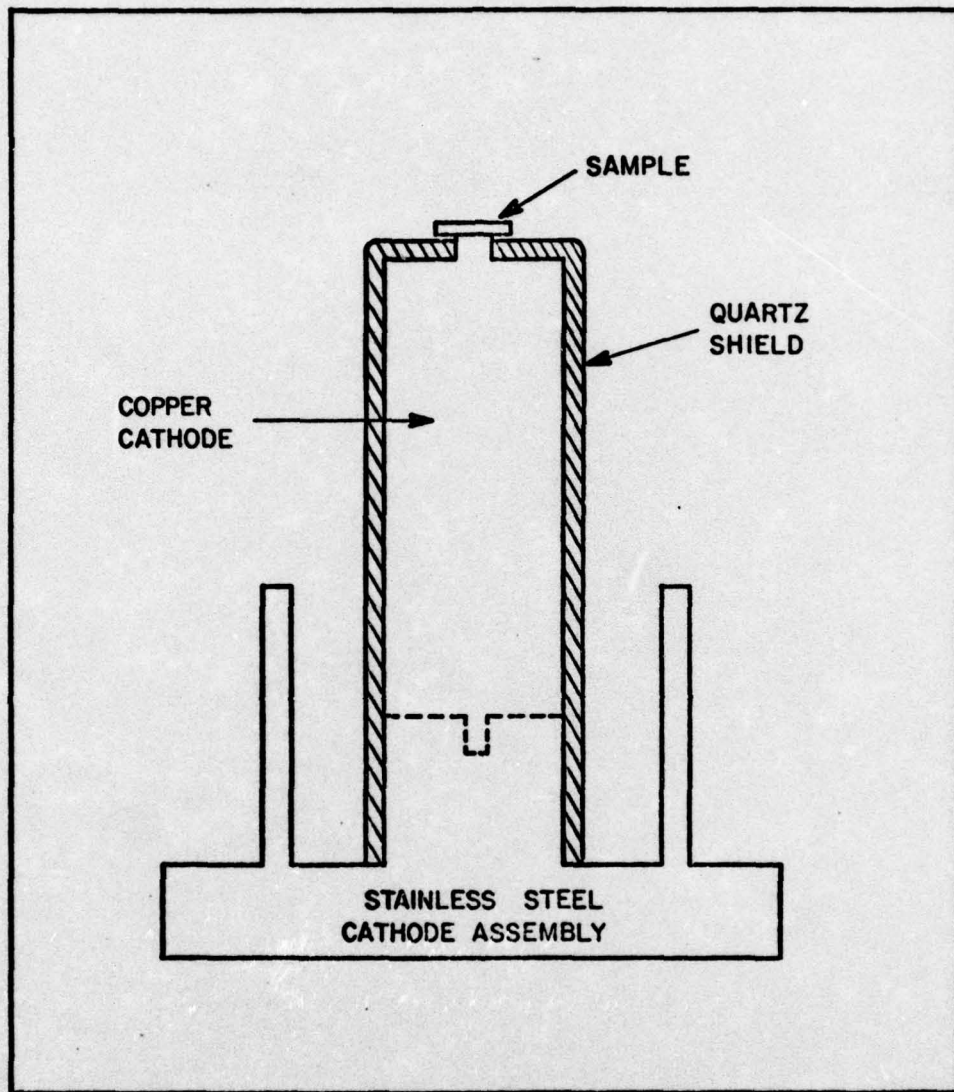


Figure 8. Sample Mounted on the Cathode of the GDOS System

the experiment by use of the leak valve. Pressure was found to remain stable to within  $\pm 1$  micron over a half hour period at a constant flow rate.

The abnormal glow discharge was started by applying a high dc potential between the electrodes and current was monitored on the ammeter in the discharge circuit.

The discharge luminescence just above the sample was focused onto the entrance slit of the monochromator by use of a quartz lens. A spherical mirror opposite the chamber window was used to increase the amount of collected light focused on the slit. Typical slit widths used were 50 microns for identifying emission lines and up to 200 microns for monitoring a particular line while profiling.

Light output from the monochromator was focused onto the RCA C31034A Quantacon photomultiplier tube after passing through the quartz-windowed chamber located inside the cooled photomultiplier housing. The tube was cooled to reduce thermal noise, which had been a problem with an uncooled RCA 1P28 tube. The tube had a high gain and quantum efficiency in the ultraviolet and visible spectral regions which made it well suited for this experiment.

Output from the photomultiplier tube was detected by one of two systems tested in this study, a photon counting or lock-in amplifier system. The photon counting system is shown schematically in Figure 7. Output from the photomultiplier tube passed through a low noise film-type 20 Kohm

anode load resistance to the amplifier/discriminator and then to the Model 1108 Multimode Processor. Output from the processor was connected to the 10 inch XY recorder where emission intensity as a function of wavelength or time was displayed.

The lock-in amplifier system is not shown, but was used as in Figure 7 with the PAR Model 124A Lock-In Amplifier replacing the photon counter, the PAR Model 221 and Model 116 preamplifiers replacing the amplifier/discriminator, and the PAR Model 191 Variable Speed Light Chopper placed in front of the entrance slit of the monochromator.

#### Determination of the Best Impurity Emission Lines

A prerequisite for measuring impurity profiles in GaAs using GDOS was the selection of a strong emission line, corresponding to the particular implanted impurity, which had no interfering lines nearby. This was accomplished by first researching spectral tables for the location of the best lines of interest (Ref 27). Then the spectral regions containing these lines were scanned and the spectra recorded while sputtering a GaAs sample which contained none of the impurity.

A second scan of the same spectral regions was then made under the same sputtering conditions, but with a pure sample of the impurity of interest or a GaAs sample doped with the impurity. The recorded spectra from these two runs were then superimposed. The exact location and strength of

the impurity spectral line and its proximity to other spectral lines were determined. This procedure was used for several of the best spectral lines of each impurity. The spectral line then selected for each impurity was that one which had the strongest intensity and which had the least interference from other spectral lines.

Spectral lines resulting from gases were determined from the use of different spectral tables (Ref 16). Molecular spectral tables were used in some cases (Ref 23).

#### Determination of Sputtering Rate and Sputtering Uniformity

The sputtering rate of the target substrate must be known in order to measure impurity profiles using the GDOS technique. Additionally, the sample should sputter uniformly for accurate results. Methods were devised in this investigation to measure sputtering rates in GaAs and uniformity in sputtering.

Sputtering Rate Studies. The method devised to measure sputtering rates was to cover part of the sample surface with aluminum foil, and sputter the sample for a fixed period of time, usually five or ten minutes. After sputtering, the foil was removed and the sputtered step was measured using the Dektak surface profiling system. The average sputtering rate was then calculated by dividing the average step height by the sputtering time. Typical sputtered step measurements are shown in Figure 9.

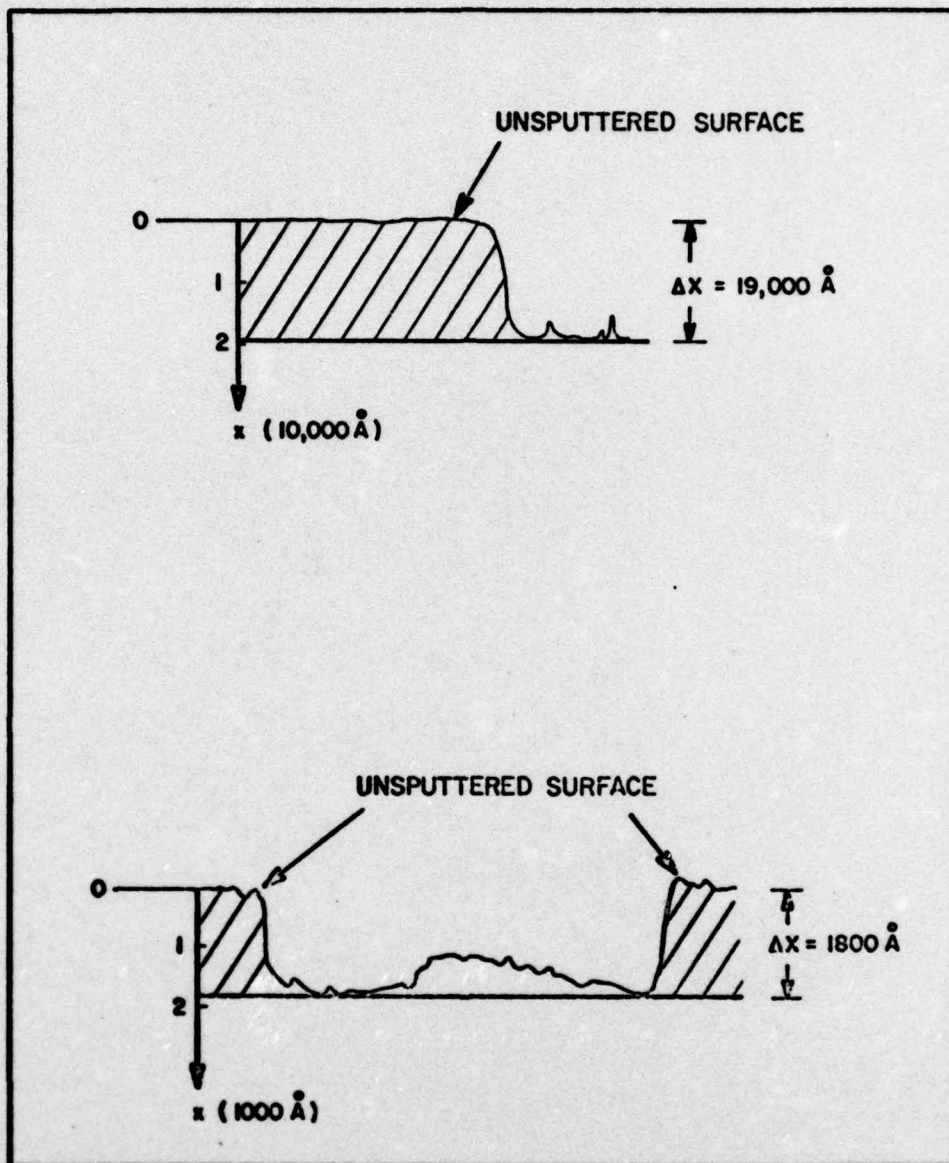


**Figure 9. Sputtered Step Heights Measured by the Dektak System**

The effect of voltage on the sputtering rate was studied by keeping the pressure constant at 50 microns and measuring the sputtering rates for various voltages between 1000 and 2000 volts. Likewise the effect of pressure on the sputtering rate was studied by keeping the voltage constant at 1000 volts and measuring the sputtering rates for various pressures between 50 and 100 microns.

Along with these studies, another study was made to determine if the intensity of a spectral line was a good indication of the sputtering rate of the target substrate. This was done by measuring the intensity of the gallium 4172.1 Å spectral line as a function of voltage from 1000 to 2500 volts at a constant pressure. Since the sputtering rate had already been measured as a function of voltage, by comparing the sputtering rate to intensity at each voltage, a correspondence between intensity and sputtering rate could be determined.

Sputtering Uniformity. Initially it was assumed that the sample surface sputtered fairly uniformly. This was supported by visually studying the sample as it was sputtered, and from the data obtained using the Dektak, which indicated that the area not covered by aluminum foil was evenly sputtered. However, an experiment was devised to confirm whether or not there indeed was uniform lateral sputtering. In this experiment, a 1000 Å thick copper film was evaporated onto the surface of a 5.0 x 3.0 mm GaAs sample. The sample

was then sputtered at 2000 volts and 70 microns of pressure. The Ga 4172.1 Å line intensity was recorded as a function of time to determine how uniformly the copper film was sputtered off, exposing the GaAs substrate.

A study was also made to determine the duration of any transient period which might be encountered when the discharge was first started. This was accomplished by monitoring the intensity of the Ga 4172.1 Å line as a function of time while sputtering a GaAs sample at 1400 volts and 70 microns.

#### Calibration of the GDOS System

For the GDOS measured impurity profiles to be meaningful, the system must be calibrated. The desired method of calibrating the GDOS system is to measure the intensity of the strong emission line of the desired impurity while sputtering bulk doped GaAs containing known concentrations of the impurity. The resulting intensity measurements would be used as standards for various impurity concentrations.

Unfortunately, bulk doped GaAs containing cadmium, zinc, and magnesium were not available in high concentrations, except for a  $8 \times 10^{18} \text{ cm}^{-3}$  Zn doped sample and a  $3.9 \times 10^{17}$  Cd doped sample, both made by the Laser Diode Laboratories. An attempt was made to calibrate the system by measuring the intensity of an emission line corresponding to an impurity implanted at various concentrations in

GaAs samples. By relating the measured peak intensities to the probable LSS peak concentrations, the system could be roughly calibrated.

### Impurity Profiles

Impurity concentration profiles were measured by monitoring a strong emission line of the particular impurity while the sample was sputtered. In these studies, the Cd 3610.5 Å line, the Zn 4810.5 Å line and the Mg 5183.6 Å lines were used for these particular dopants.

Some gallium implanted silicon samples were also studied since the material was available and the Ga 4172.1 Å line was a good one for monitoring. The sputtering rate of silicon was measured for the sputtering parameters used.

The profiles were calculated by plotting the intensity of the spectral line, corresponding to the implanted impurity, as a function of time and then combining this with the known sputtering rate of the substrate material. The result is a concentration profile with concentration plotted as a function of depth into the substrate.

A series of profile runs were made on GaAs samples implanted with fluences of  $10^{14}$ ,  $10^{15}$ , and  $10^{16}$  ions/cm<sup>2</sup>. Profile runs were made using Mg implanted at fluences of  $10^{15}$ , and  $5 \times 10^{15}$  ions/cm<sup>2</sup> which corresponded to peak concentration of  $8.5 \times 10^{19}$  ions/cm<sup>3</sup> and  $4.2 \times 10^{20}$  ions/cm<sup>3</sup> respectively. Profile runs were made using Ga

ions in silicon at a fluence of  $10^{15}$  ions/cm<sup>2</sup> which corresponded to a peak concentration of  $1.6 \times 10^{20}$  ions/cm<sup>3</sup>.

An attempt was made to cap the GaAs samples with a 400-500 Å layer of Si<sub>3</sub>N<sub>4</sub>, so that steady state sputtering would be achieved before sputtering of the implanted substrate began, thus providing more accurate results.

The results of these experiments are discussed in Chapter V.

## V. Results and Discussion

The results of the GDOS investigation are presented and discussed in this chapter. The data are analyzed with respect to the following areas.

1. Investigation of the discharge spectrum.
2. Investigation of sputtering rate parameters.
3. Investigation of sputtering uniformity.
4. Investigation of GDOS impurity profiling.

### Investigation of the Discharge Spectrum

The discharge spectrum contained many strong argon emission lines and numerous weaker emission lines corresponding to impurities in the discharge gas or the electrodes.

By superimposing spectra as discussed in Chapter IV, the best emission lines for cadmium, zinc, and magnesium were found to be: Cd 3610.5 Å, Zn 4810.5 Å, and Mg 5183.6 Å. The superimposed spectra for these dopants are shown in Figures 10, 11, and 12 respectively.

### Investigation of Sputtering Rate Parameters

The effects of voltage and pressure on the sputtering rate of GaAs were measured using the Dektak and sputtered step method described in Chapter IV. This method was fast and it is believed that error is limited to the estimation of the average sputtering step height and the effects of the rough sputtered surface on the Dektak stylus. Combined error was estimated to be less than 20 per cent.

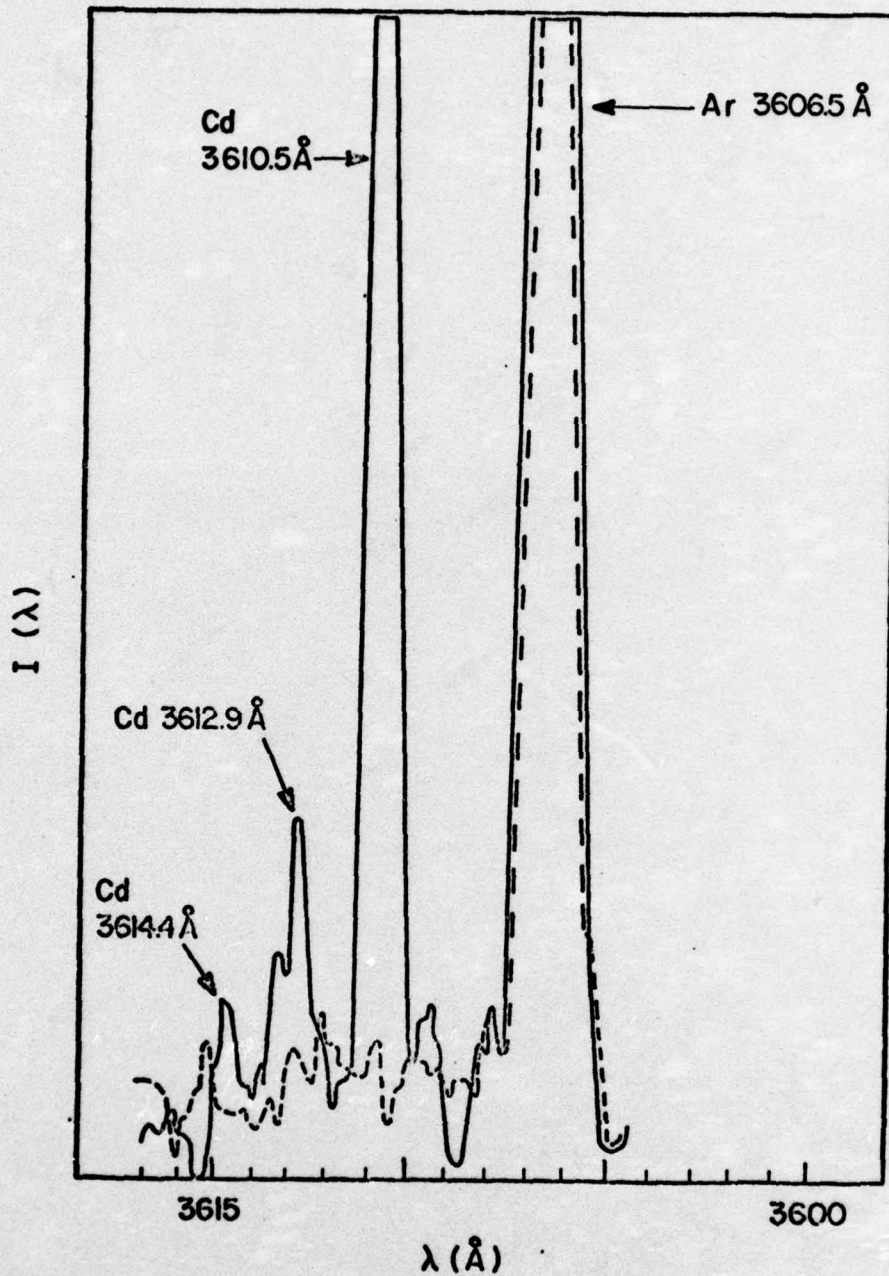


Figure 10. Spectrum From Sputtered Cadmium (Solid Line) Superimposed on Spectrum of Undoped GaAs (Broken Line)

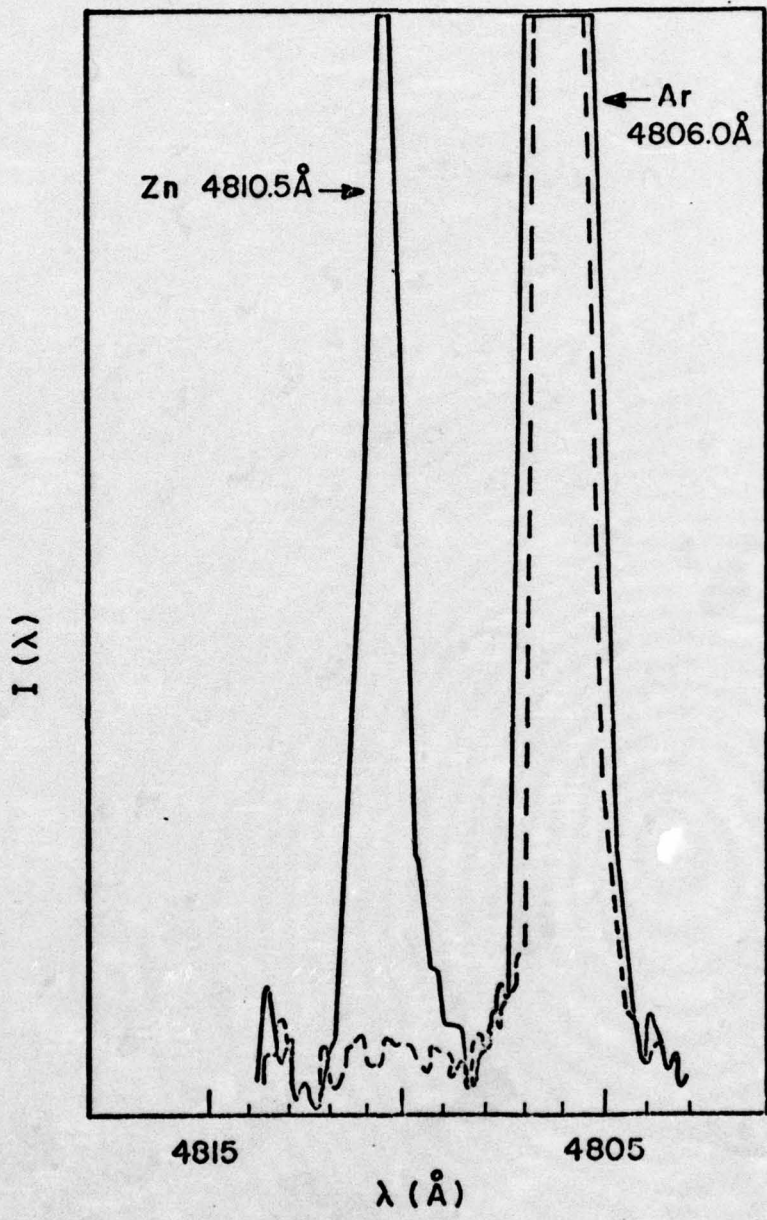


Figure 11. Spectrum From Sputtered Zinc (Solid Line) Superimposed on Spectrum of Undoped GaAs (Broken Line)

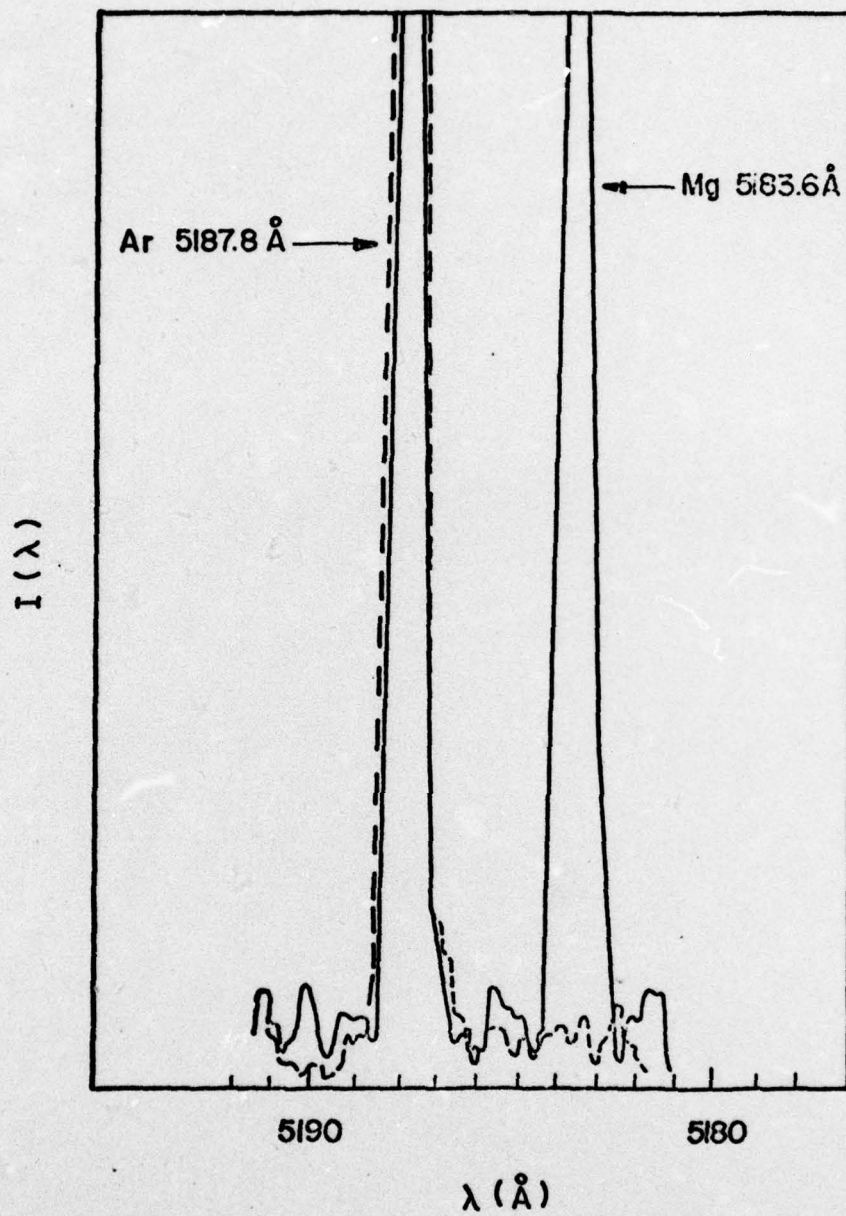


Figure 12. Spectrum From Sputtered Magnesium (Solid Line) Superimposed on Spectrum of Undoped GaAs (Broken Line)

Effect of Voltage on Sputtering Rate. The sputtering rate in GaAs was found to increase rapidly with increasing voltage at a constant gas pressure of 50 microns. This agrees with theory. Tabulated values of measured sputtering rates as a function of voltage are given in Table I and are plotted in Figure 13.

Table I  
Sputtering Rate Versus Voltage

<u>Voltage (volts)</u>	<u>Sputtering Rate (Å/min)</u>
1000	300
1200	500
1500	850
1500 *	950
2000	2400

\* Independent measurements were made at 1500 volts

Effect of Pressure on Sputtering Rate. The sputtering rate was found to be fairly insensitive to pressure variation at 1000 volts. Sputtering rate only increased slightly with increasing gas pressure up to about 80 microns, then decreased. This does not agree with theory but could be a result of measurement errors or the low sputtering voltage used. Tabulated values of measured sputtering rates as a function of gas pressure, at constant 1000 volts, are given in Table II and are plotted in Figure 14.

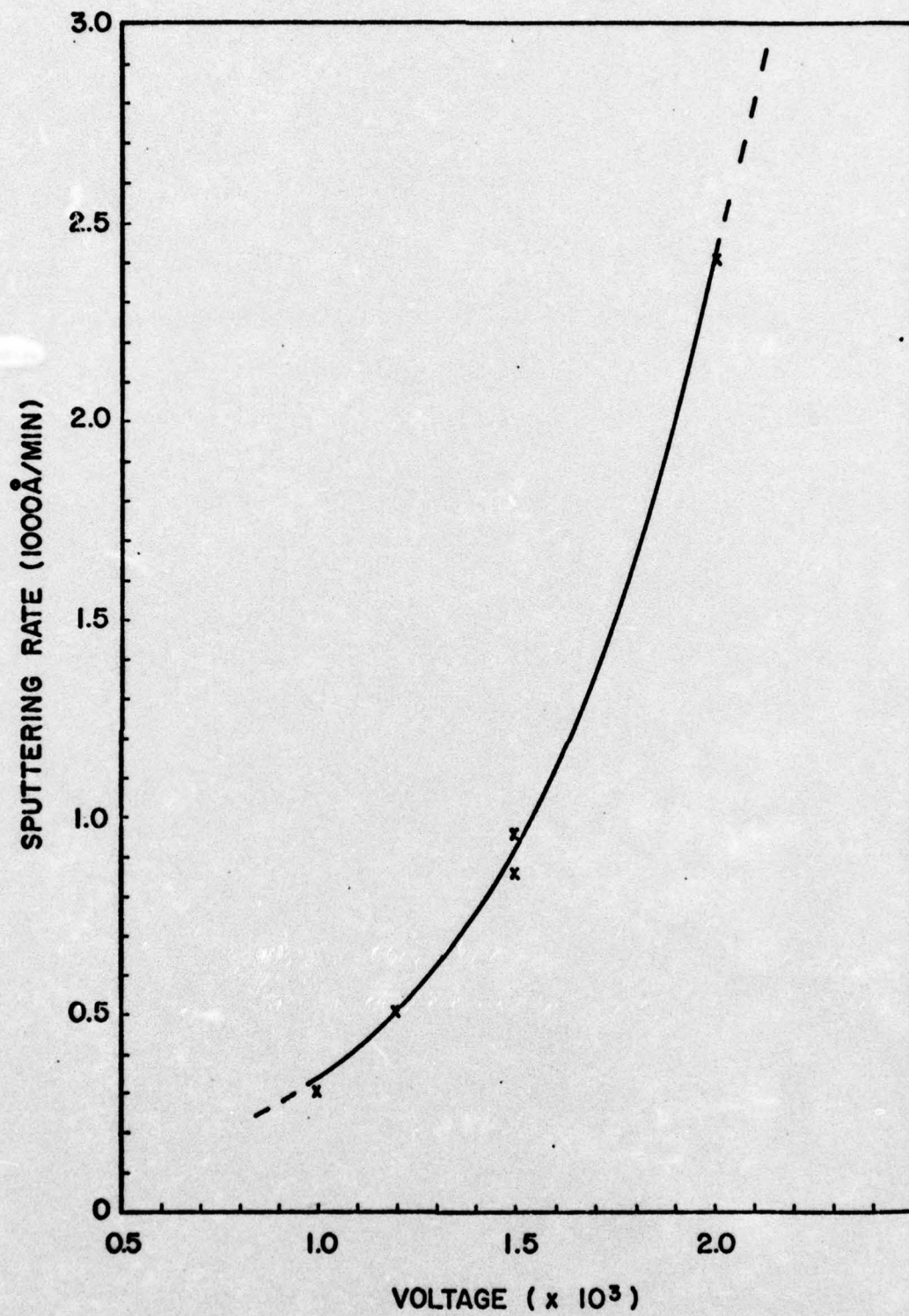


Figure 13. Sputtering Rate Versus Discharge Voltage

Table II

Sputtering Rate Versus Gas Pressure

<u>Pressure (microns)</u>	<u>Sputtering Rate (Å/min)</u>
50	200
60	150
65	300
75	300
85	400
100	300

Correspondence Between Sputtering Rate and Emission Intensity. Experiments, described in Chapter IV, showed that the sputtering rate was almost directly proportional to the intensity of a monitored emission line. The intensity of the Ga 4172.1 Å line was measured as a function of voltage at a constant gas pressure and the resulting intensity was then plotted versus the previously measured sputtering rate for various voltages.

The tabulated values of gallium line intensity versus voltage are given in Table III and plotted in Figure 15. The relationship between intensity and sputtering rate is then plotted in Figure 16.

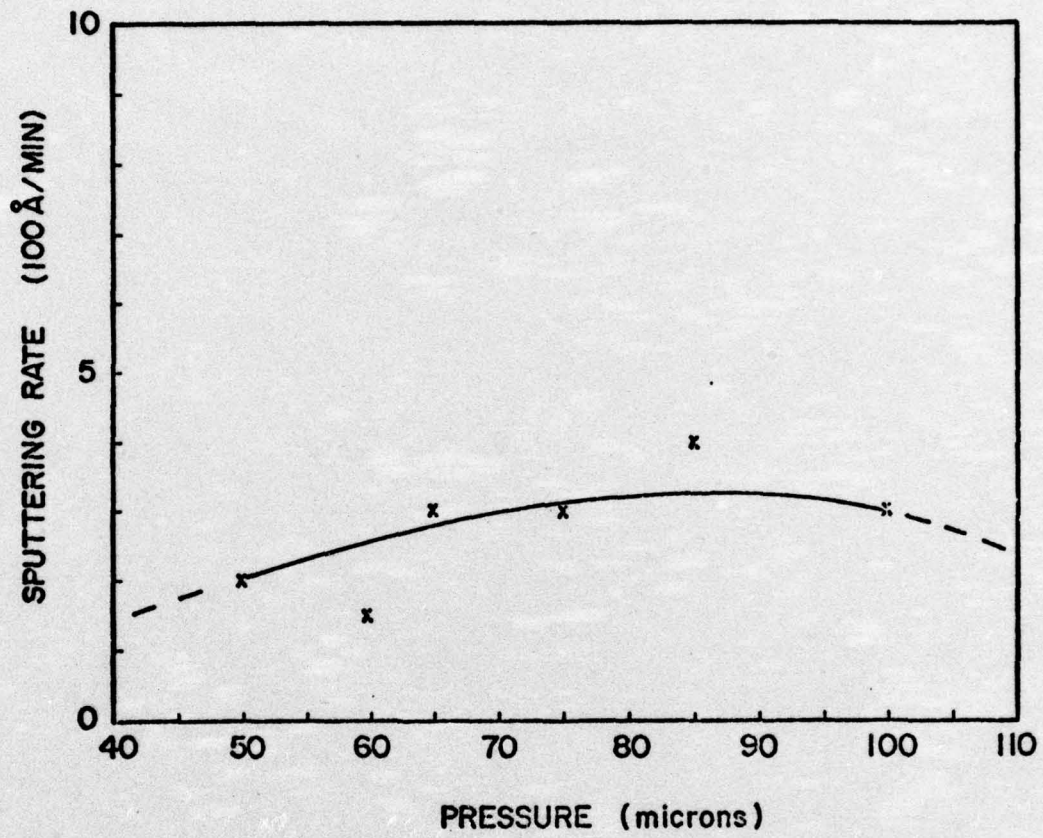


Figure 14. Sputtering Rate Versus Discharge Pressure

Table III

## Emission Intensity Versus Voltage

<u>Voltage (volts)</u>	<u>Intensity *</u>	<u>Voltage (volts)</u>	<u>Intensity *</u>
1000	0.08	1800	1.20
1100	0.14	1900	1.70
1200	0.23	2000	2.20
1300	0.35	2100	2.80
1400	0.34	2200	3.60
1500	0.44	2300	4.60
1600	0.64	2400	5.90
1700	0.86	2500	6.60

\* Arbitrary Units

#### Investigation of Sputtering Uniformity

As a result of the sputtering step studies done with the Dektak and the experiment in which a 1000 Å layer of copper was sputtered from a GaAs sample, it was determined that sputtering was non-uniform across the sample surface. Dektak studies revealed that sputtered areas had sharp vertical steps and fairly uniform sputtered depth across the sample, as was shown previously in Figure 9.

The sample was assumed to sputter fairly uniformly across its whole surface. However, when the copper coated sample was sputtered, it was found that the sample was not sputtered around its edges, as shown in Figure 17. This lack of sputtering at the edges of the sample is in sharp

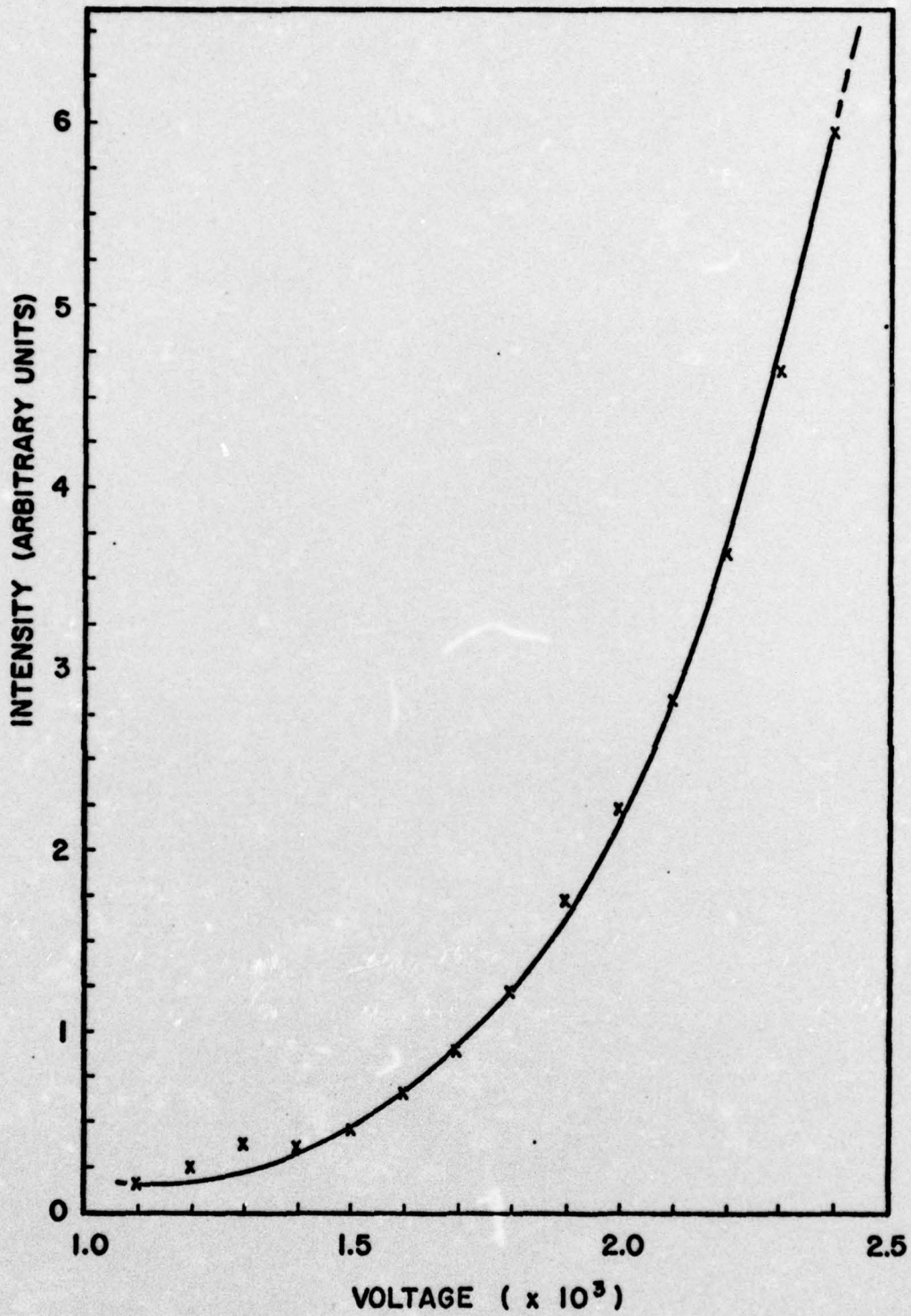


Figure 15. Intensity of Ga 4172.1 Å Emission Line Versus Discharge Voltage

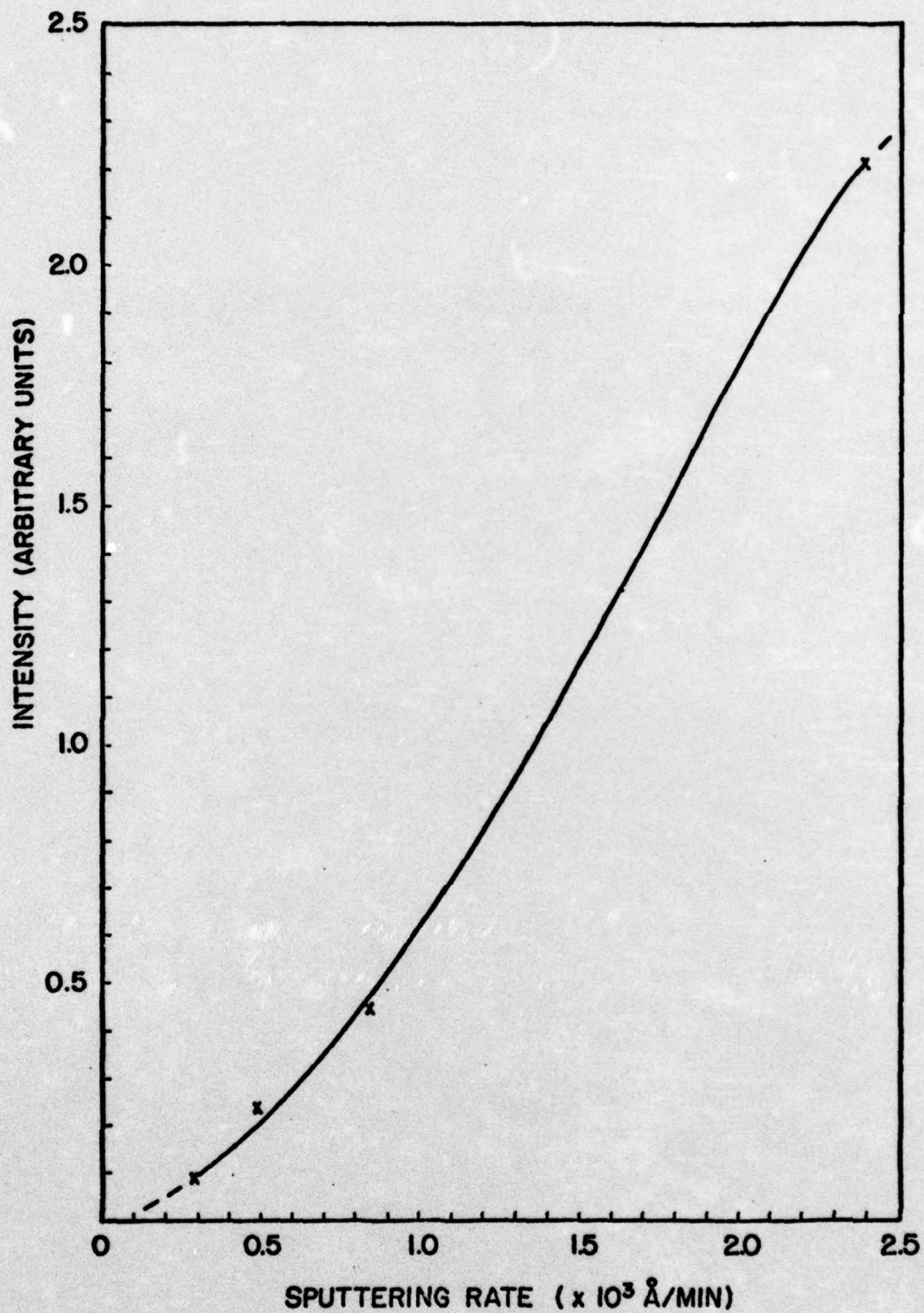


Figure 16. Intensity of Ga 4172.1 Å Emission Line Versus Sputtering Rate

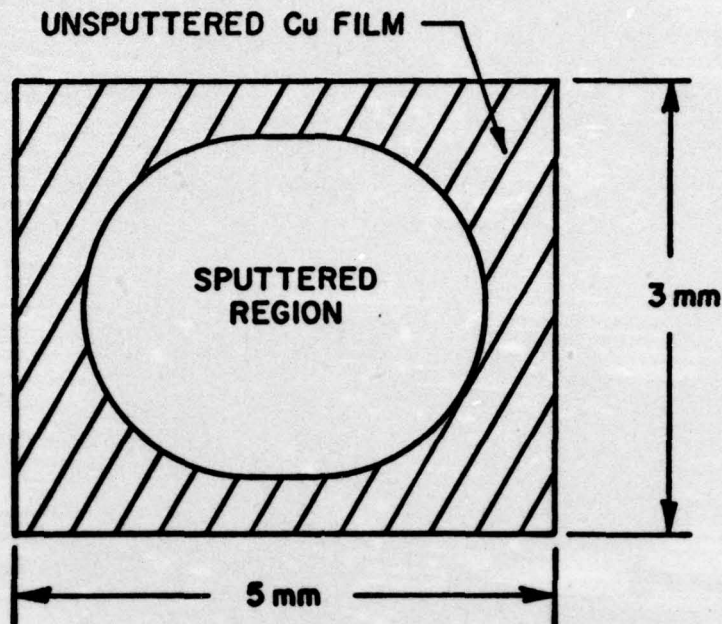


Figure 17. Non-Uniform Lateral Sputtering of a GaAs Sample

disagreement with what had been expected from theory and reported by others (Ref 11:2707). Sharp edges were expected to cause high local current densities and strong electric fields near them, thus leading to increased sputtering at the edges. This sputtering pattern and non-uniformity is now thought to be a direct result of the cathode/target geometry used in the experiment.

In this experiment, the intensity of the Ga 4172.1 Å line was plotted as a function of sputtering time as shown in Figure 18. The gradual increase in intensity of the gallium line rather than a sharp increase also indicated

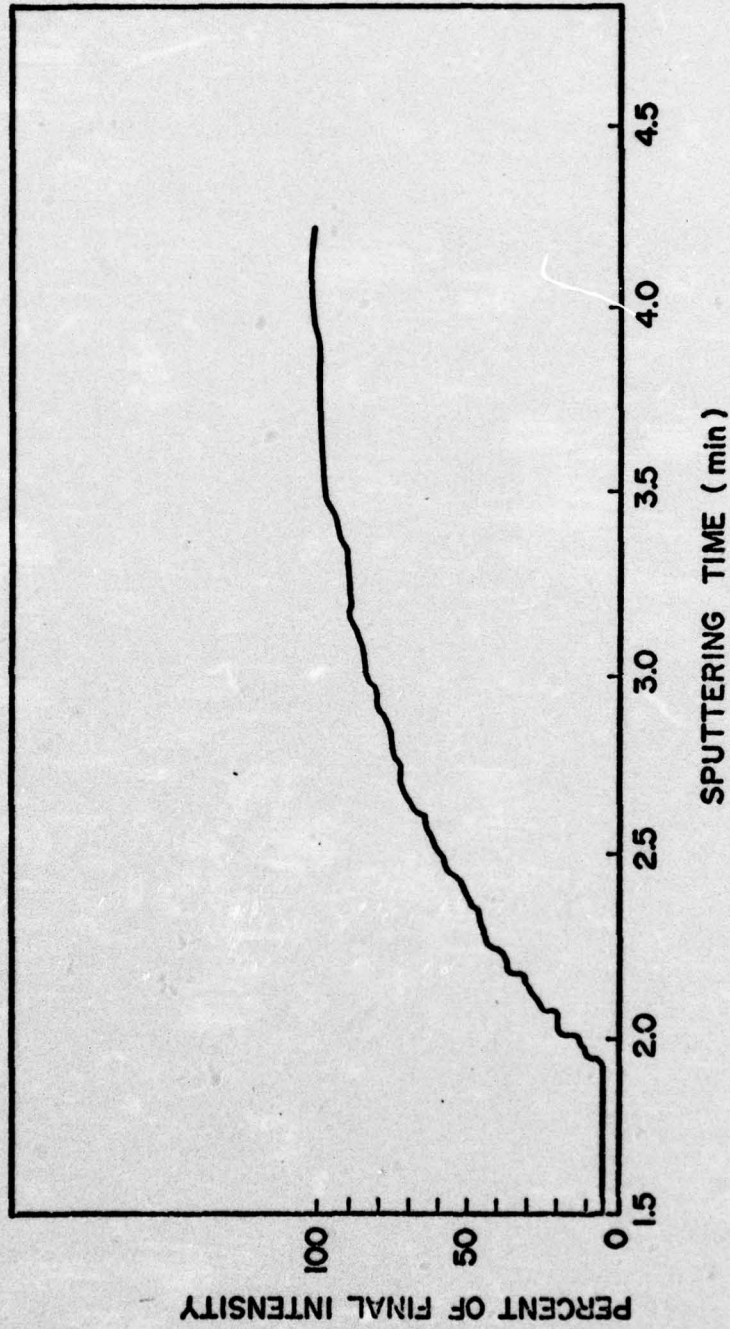


Figure 18. Intensity of Ga 4172.1 Å Emission Line as Copper Film was Sputtered

that the lateral sputtering was non-uniform using this cathode/target geometry.

The discharge was found to have a non-steady period, lasting for about 20 seconds. This was the typical time to reach within 10 per cent of its final steady-state sputtering rate. This result was found from the experiment in which the intensity of the Ga 4172.1 Å line was measured as a function of time after sputtering was started. Figure 19 shows the resulting plot. This figure also shows that the steady-state intensity fluctuates at about five per cent or less.

#### Investigation of GDOS Impurity Profiling

Calibration of the GDOS System. The GDOS system was not calibrated because of the unavailability of the required impurity concentrations in bulk doped GaAs samples. One Zn doped sample was available however, which had a concentration of  $8 \times 10^{18}$  ions/cm<sup>3</sup>. It was found that the zinc was detectable, but only while sputtering at 2500 volts and 70 microns, which corresponded to a sputtering rate of over 2500 Å/min. Figure 20 shows the 4722.2 Å Zn line in the bulk doped GaAs sample at the sputtering parameters just mentioned. Its spectrum is superimposed on a spectrum made using the same sputter discharge parameters, but while sputtering a GaAs sample containing no zinc. Figure 21 then shows the superimposed spectra for the GaAs containing no zinc and a spectra made of the same region while sputtering a pure sample of zinc at 2000 volts and 70 microns.

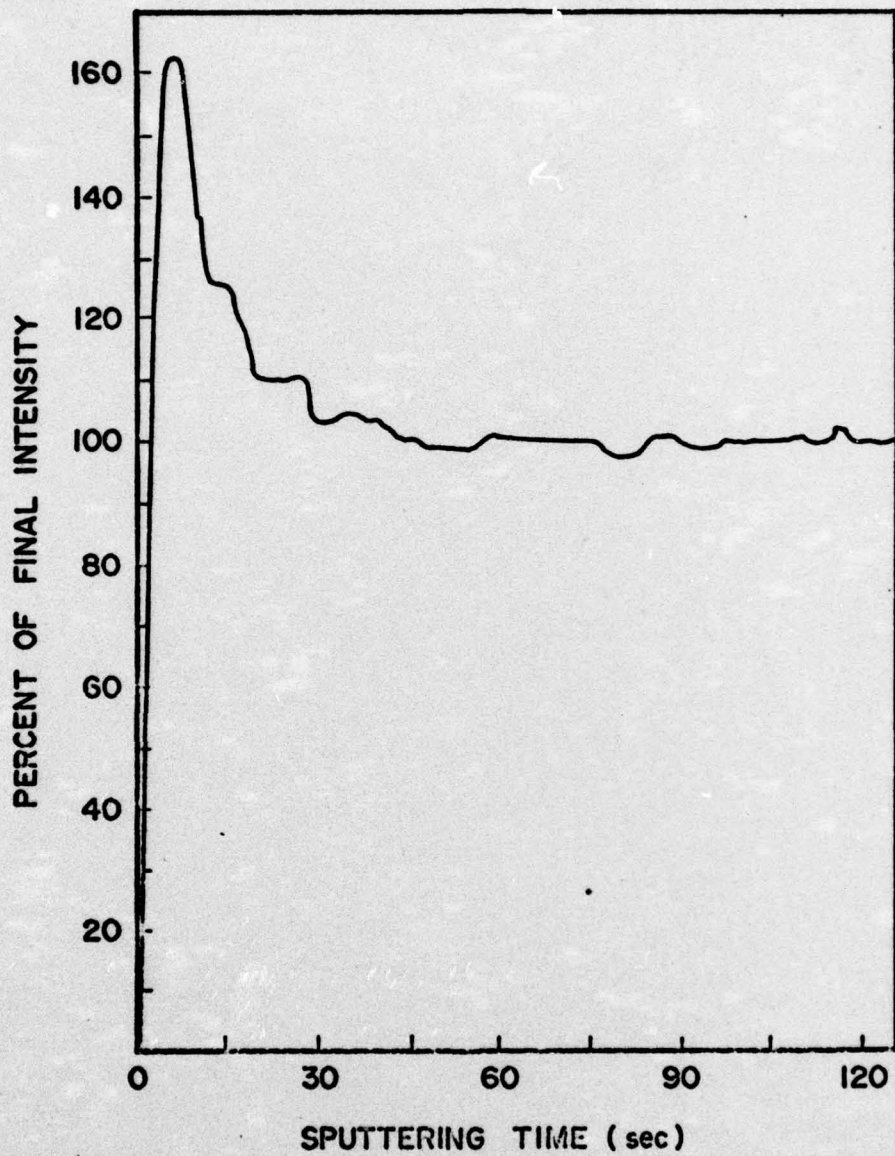


Figure 19. Intensity of Ga 4172.1 Å Emission Line During Initial Transient Period of the Discharge

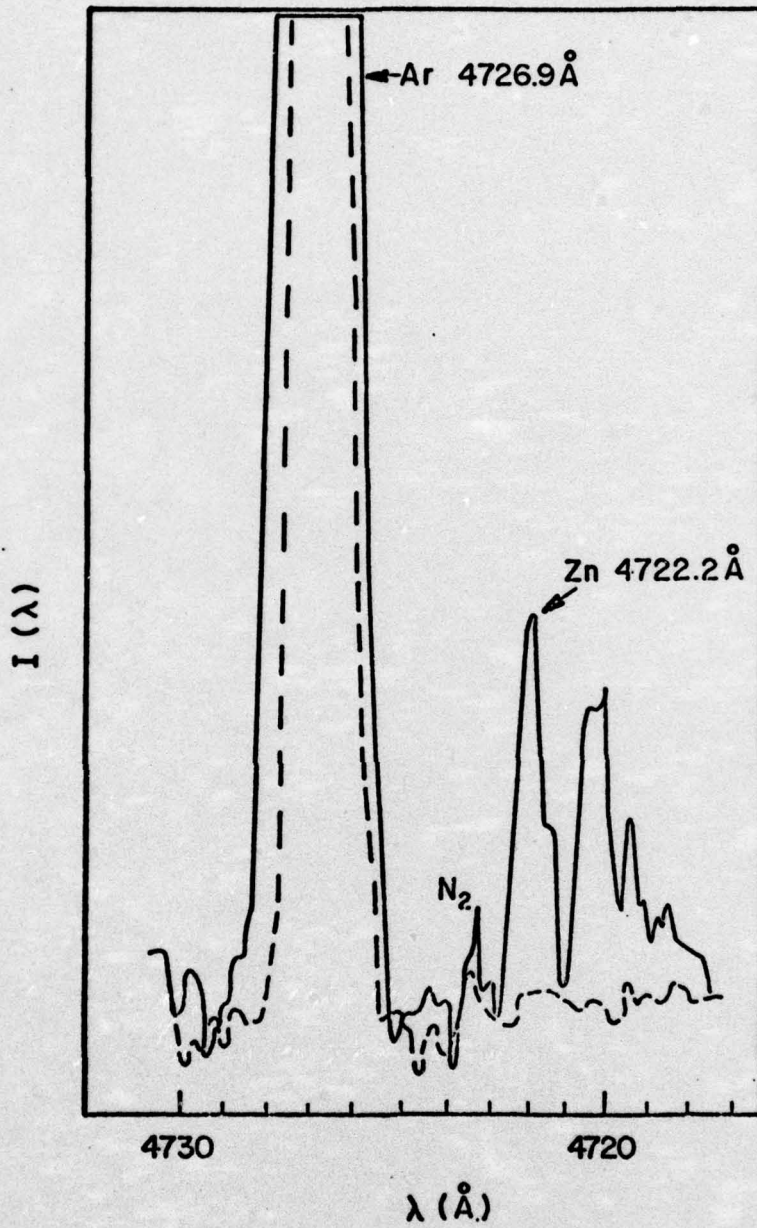


Figure 20. Spectrum From Sputtered  $8 \times 10^{18}$  ions/cm<sup>3</sup> Zinc Doped GaAs (Solid Line) Superimposed on Spectrum of Undoped GaAs (Broken Line)

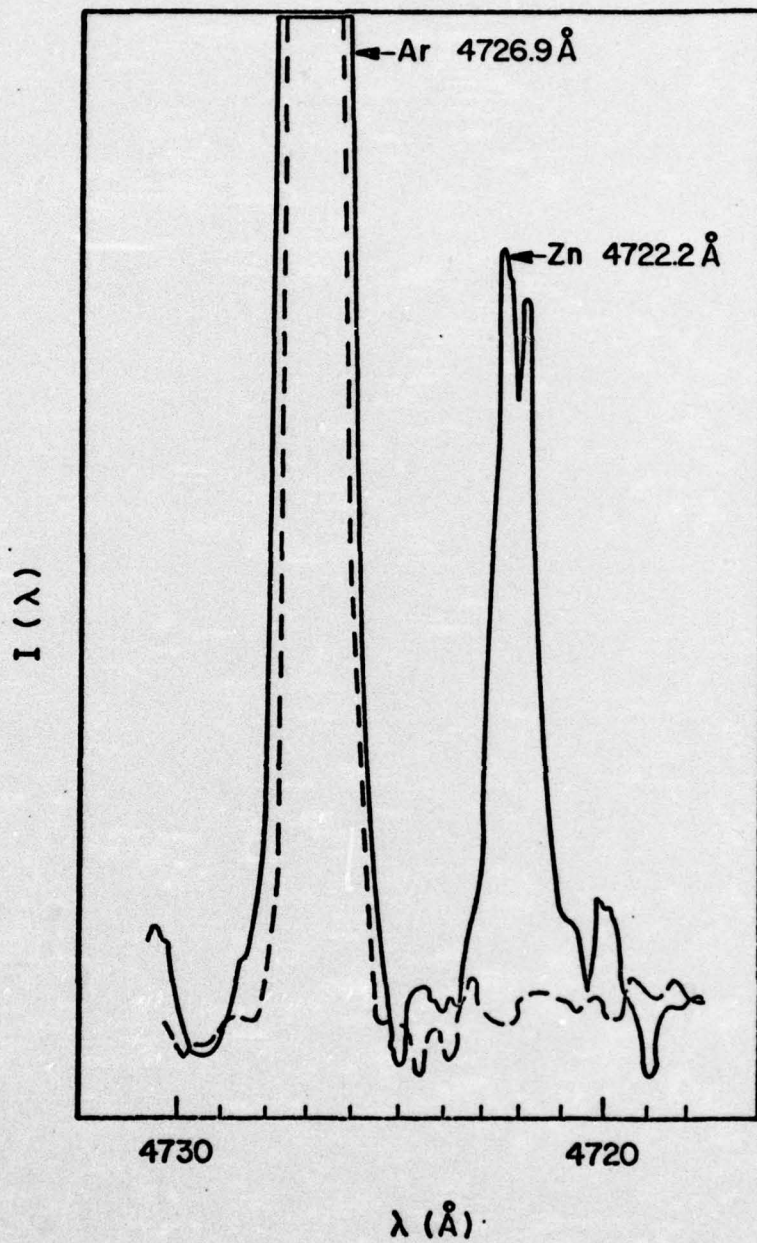


Figure 21. Spectrum From Sputtered Zinc (Solid Line) Superimposed on Spectrum of Undoped GaAs (Broken Line)

The GDOS system could not be calibrated by using a correspondence between peak intensity of the impurity emission line and the peak concentration of implanted impurity in GaAs because only peak concentrations of about  $10^{21} \text{ cm}^{-3}$  were detectable. This resulted from the fact that the impurity emission lines in the discharge were weak, even when pure samples of the impurity were sputtered.

Impurity Profiles. Uncalibrated impurity profiles were measured for zinc and magnesium implanted in GaAs and gallium implanted in silicon. Attempts to obtain impurity profiles for cadmium in GaAs were unsuccessful. Due to impurity line weakness, 200 micron entrance slit widths were used for all profile measurements except Ga in silicon in which the slit width used was 75 microns. Additionally, high sputtering rates had to be used for the Cd, Zn, and Mg profiles to increase emission intensities, which resulted in profile calculation errors, estimated to be as high as 35 per cent.

Attempts to cap the samples in order to attain steady-state sputtering prior to sputtering the implanted substrate were unsuccessful. Studies which were made using samples of Cd implanted GaAs, capped with a 400-500 Å layer of  $\text{Si}_3\text{N}_4$ , resulted in misleading Cd profiles. The Cd 3610.5 Å line being monitored, using a 200 micron slit, was masked by the strong molecular spectral line of either  $\text{N}_2$  or NH at 3612.4 Å and 3609.6 Å respectively. This cap also resulted

in unstable sputtering, since it was an insulating material. Figure 22 shows the effect of the  $\text{Si}_3\text{N}_4$  cap on the Cd 3610.5 Å line. The dotted line represents the intensity from the 3610.5 Å region when sputtering an undoped sample of GaAs. The solid line shows the intensity of the same region while sputtering the  $\text{Si}_3\text{N}_4$  capped, but undoped sample.

Zinc profiles were obtained for Zn implanted into GaAs at 99 keV and a fluence of  $10^{16}$  ions/cm<sup>2</sup> corresponding to a peak concentration of  $1.7 \times 10^{21}$  ions/cm<sup>3</sup>,  $R_p$  of 483 Å, and  $\Delta R_p$  of 238 Å. Below the  $10^{16}$  ions/cm<sup>2</sup> fluence, results were unreliable. Figure 23 shows the relative GDOS measured profile plotted with the LSS theoretical profile, which has been plotted on a linear scale. The profile was measured using an estimated sputter rate of 1400 Å/min as determined from Figure 13 for sputtering at 1800 volts.

Magnesium profiles were obtained for Mg implanted into GaAs at 99 keV and a fluence of  $5 \times 10^{15}$  ions/cm<sup>2</sup> corresponding to a peak concentration of  $4.2 \times 10^{20}$  ions/cm<sup>3</sup>,  $R_p$  of 910.5 Å and  $\Delta R_p$  of 471.2 Å. Below this fluence, results were unreliable. Figure 24 shows the relative GDOS measured profile plotted with the LSS theoretical profile, which has been plotted on a linear scale. The profile was made at a sputtering voltage of 1750 volts and the sputtering rate was estimated to be 1700 Å/min.

Gallium profiles were obtained for Ga implanted into

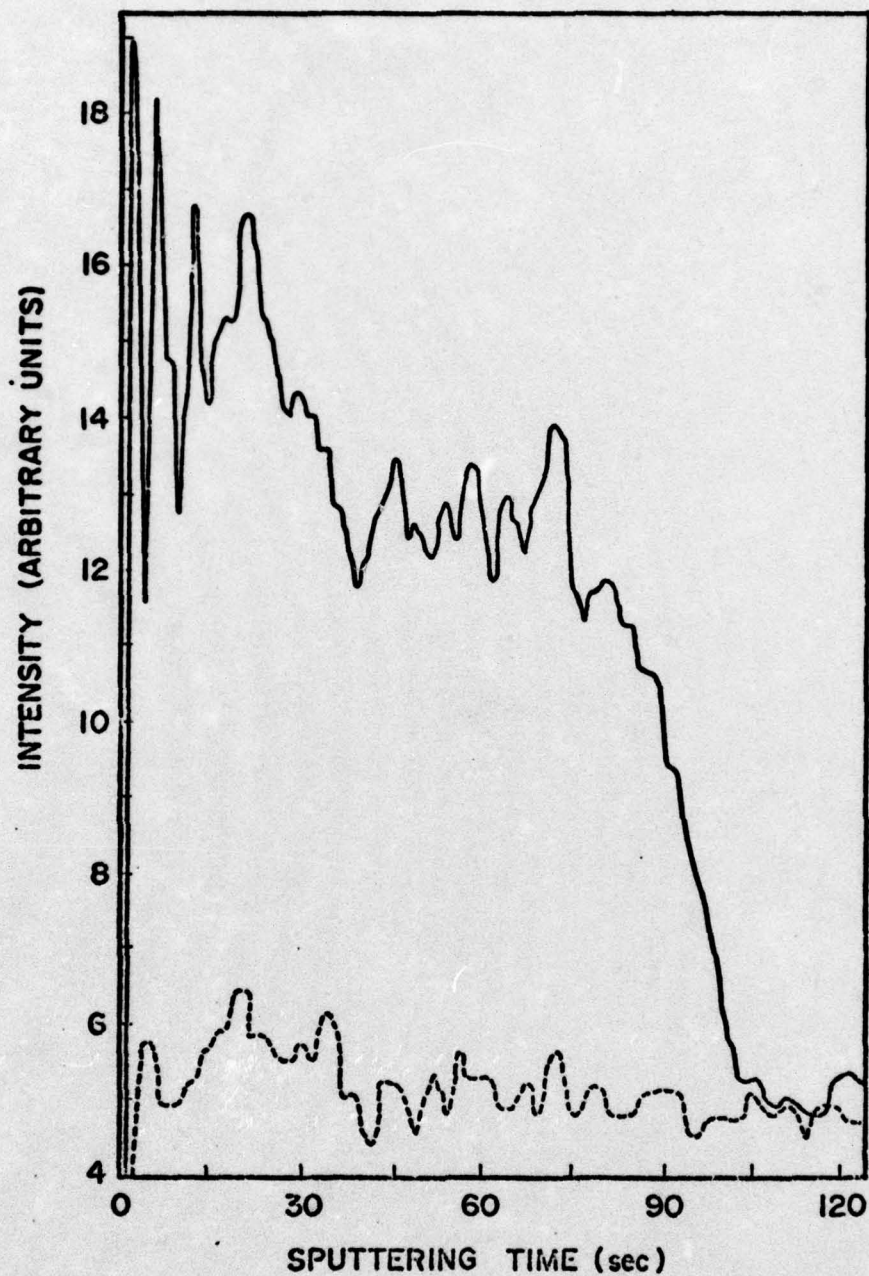


Figure 22. Effects of Sputtering  $\text{Si}_3\text{N}_4$  Cap (Solid Line) on GaAs Versus Uncapped GaAs (Broken Line) While Monitoring the Cd 3610.5 Å Emission Line

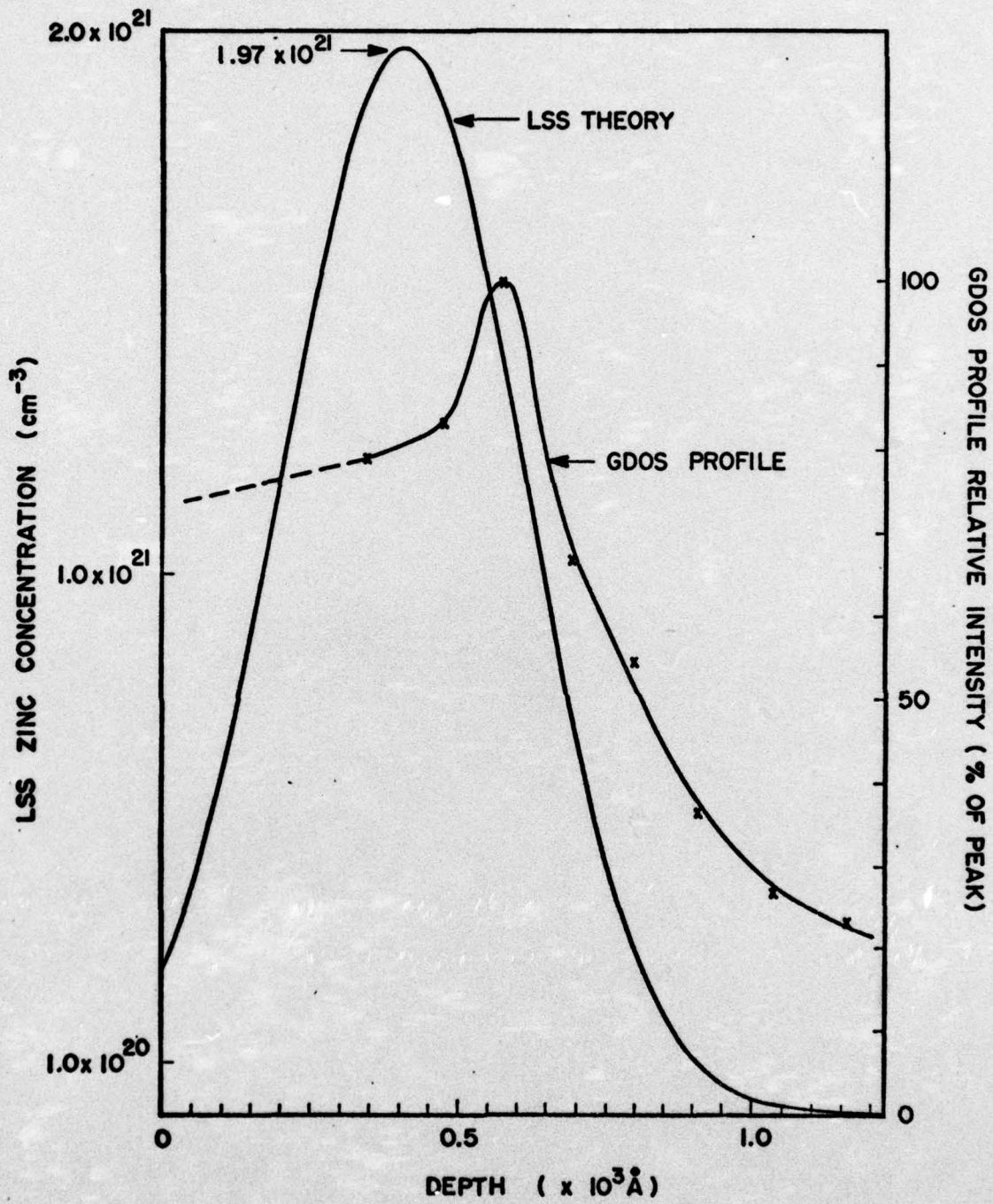


Figure 23. Relative GDOS Measured Profile of Zinc Implanted GaAs Compared to Theoretical LSS Profile

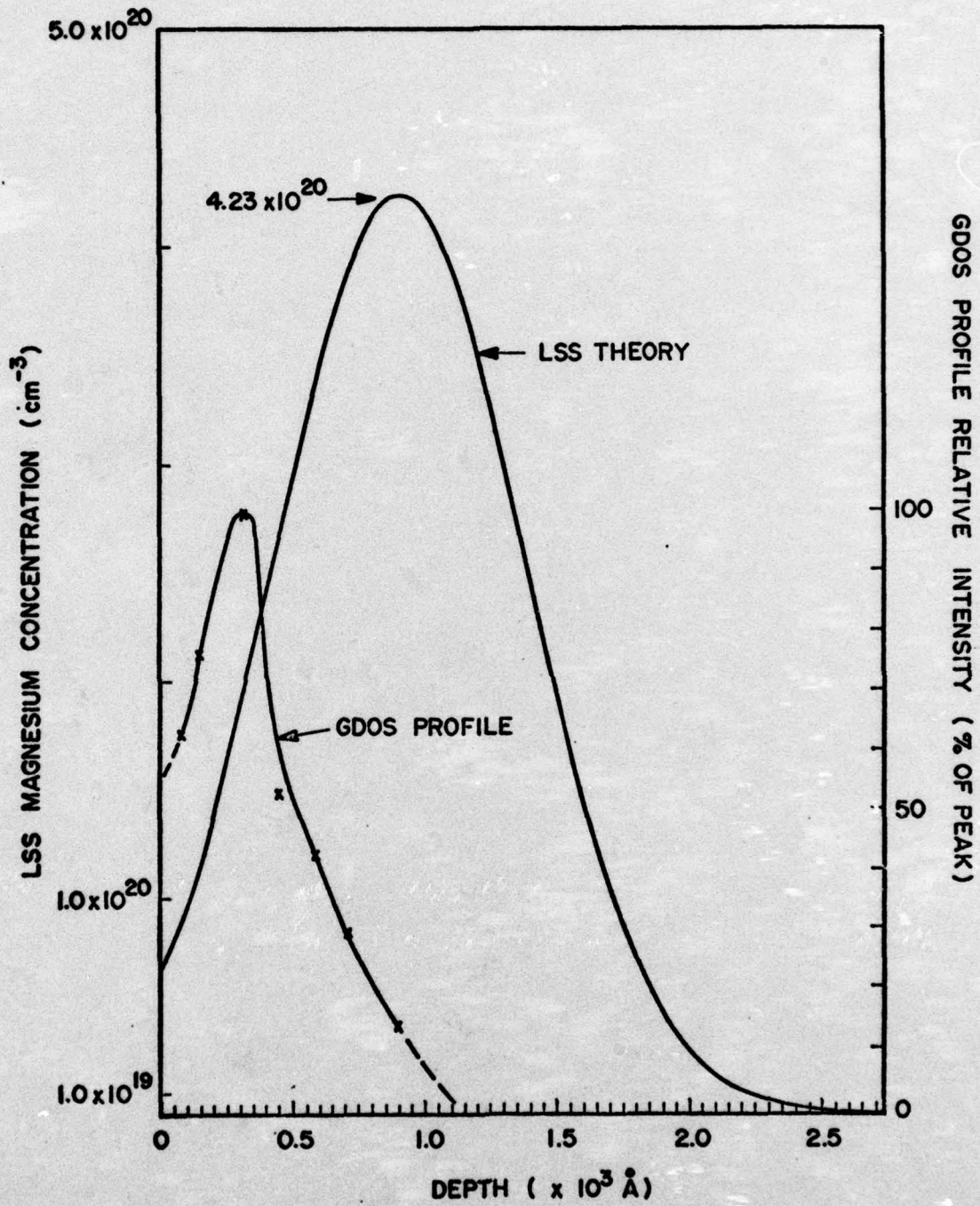


Figure 24. Relative GDOS Measured Profile of Magnesium Implanted GaAs Compared to Theoretical LSS Profile

silicon at 120 keV and a fluence of  $10^{15}$  ions/cm<sup>2</sup> corresponding to a peak concentration of  $1.6 \times 10^{20}$  ions/cm<sup>3</sup>, Rp of 721 Å, and ΔRp of 258 Å. Figure 25 shows the relative GDOS measured profile plotted with the ISS theoretical profile, which has been plotted on a linear scale. The profile was made at a sputtering voltage of 2000 volts and the sputtering rate was measured independently and found to be 200 Å/min at this voltage.

It is believed that sputtering rate error accounts for much of the difference between peak locations of the measured and theoretical profiles, except for the magnesium profile, which may not be implanted as deep as was expected.

The profile of implanted Ga ions in silicon shows a possible tail due to channeling of ions. This finding can be compared to similar profiles reported by Crowder, who measured the profile of 140 keV Ga ions implanted at a fluence of  $10^{15}$  ions/cm<sup>2</sup> into silicon and measured by radio chemical techniques (Ref 5:947). Those results show an extended tail beyond the ISS theoretical profile and a peak shifted to the right of the ISS peak.

Conclusions and recommendations based on the results of this investigation are presented in Chapter VI.

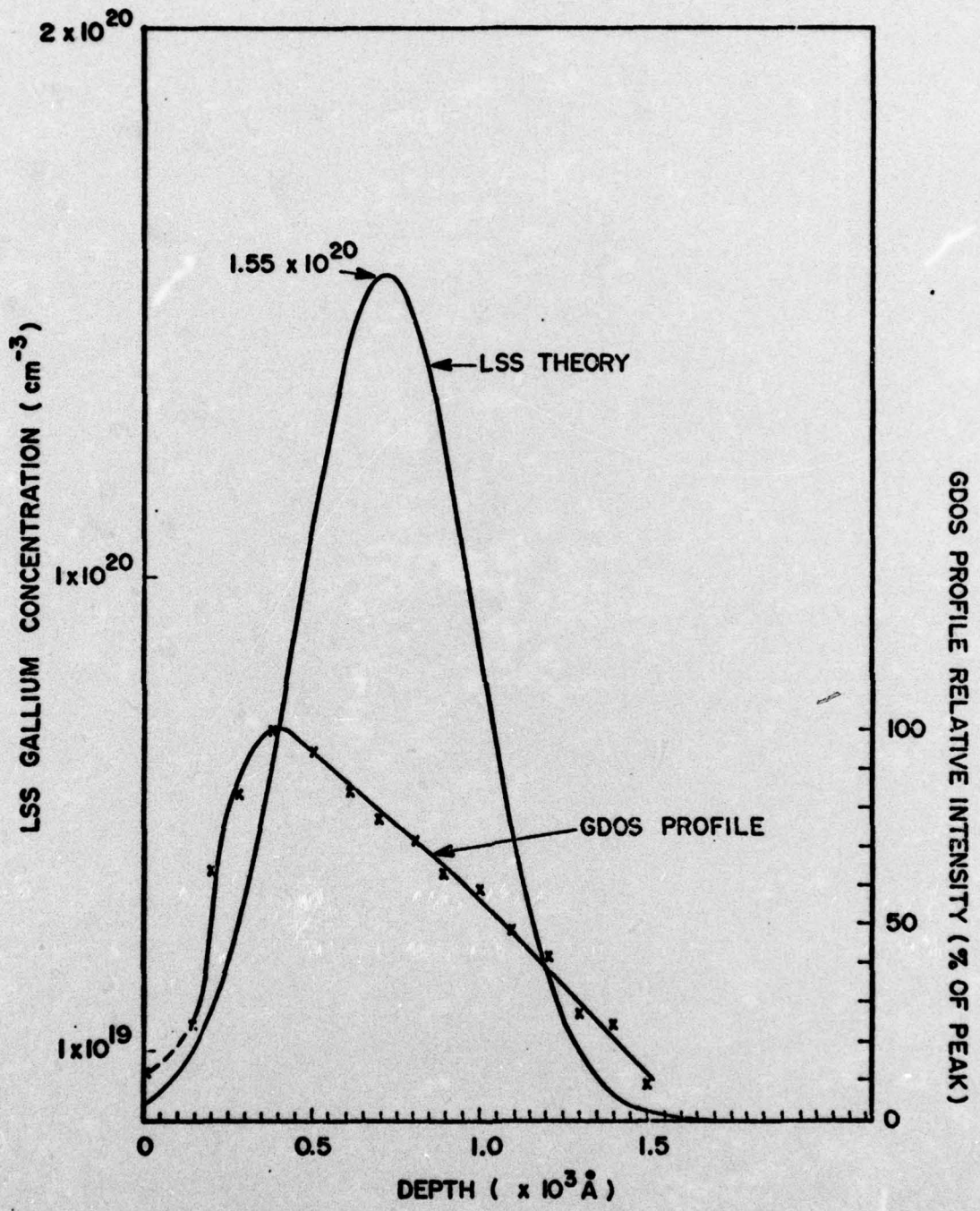


Figure 25. Relative GDOS Measured Profile of Gallium Implanted Silicon Compared to Theoretical LSS Profile

## VI. Conclusions and Recommendations

This chapter presents the author's conclusions about the investigation and his recommendations for the continuation of the GDOS study of ion implanted gallium arsenide.

### Conclusions

From the analysis of the results obtained in this investigation, the following conclusions are drawn concerning the use of the GDOS technique for total impurity profiling in unannealed GaAs. Results indicate that:

1. From the results of this study, the GDOS technique appears to be applicable to the measurement of total impurity profiles in GaAs for some implanted impurities, but improvements in the system will be required if meaningful profiles are to be obtained.
2. Results have shown that the signal strength of the impurity emission lines will have to be increased by an order of magnitude or more. Otherwise the GDOS will not be very useful since the minimum concentration detection limit will be only  $10^{19}$  to  $10^{20}$  ions/cm<sup>3</sup>. Weakness of emission lines was the single largest problem of the present system. Larger samples appear to increase emission intensity.
3. It appears that even if emission line intensities are increased sufficiently, GDOS may not be as useful for some elements as others due to the inherent weakness of

the emission lines of some elements over others and also due to overlapping of some emission lines.

4. The transient sputtering period encountered when the glow discharge was started decreased profile accuracy and must be eliminated if accurate results are to be obtained for shallow implants in GaAs.

5. Lower rates of sputtering must be used in profile measurements than were used in this investigation, if the GDOS technique is to have good depth resolution. Rates below 500 Å/min would be preferable.

6. The cathode/target geometry used in this study caused non-uniform lateral sputtering of the sample surface, and should be changed to achieve uniform surface sputtering. The results should be an increase in impurity emission line intensity and more profile accuracy. It is believed that the cathode geometry used in this study also resulted in higher sputtering rates than a plane cathode would have, under the same sputtering parameters. This is due to the fact that the geometry used in this study created a higher current density on the target surface than a plane cathode would have created.

7. Spectral line intensity appears to be almost directly proportional to the actual sputtering rate in the target substrate. It therefore can be used as a sensitive method of monitoring sputtering rates and rate variations during profiling.

8. It is felt that accurate calibration of the GDOS

system can be accomplished by using GaAs samples which are bulk doped with various concentrations of the desired impurity.

### Recommendations

This investigation has provided the foundation for further study of the GDOS impurity concentration profiling technique applied to GaAs. Qualitative and quantitative results of this study indicate that further investigations should be pursued. Further experimentation should result in increased profile accuracy, depth resolution, and lower concentration detection limits, possibly to below  $10^{18}$  ions/cm<sup>3</sup> for some impurities. The following recommendations are made for further investigations.

First, the light collection efficiency of the GDOS system should be increased in order to increase the intensity of impurity emission line signals which reach the photocathode. This should substantially increase the concentration detection limits of the system.

The light collection efficiency can be increased by replacing the experimentally designed, quartz windowed, chamber used in the cooled photomultiplier housing. It should be replaced by a commercially made chamber and lens system, or a chamber and lens system designed to focus all the light from the exit slit of the monochromator onto the photocathode.

A grating which is blazed at 2500 Å or 3000 Å should

be used when working with emission lines near these regions. Additionally, an attempt should be made to increase the light collection from the glow discharge onto the entrance slit of the monochromator by other lens systems.

It is recommended that an attempt be made to increase the efficiency of the excitation process in the discharge chamber in order to increase impurity emission line intensities. This could be done by using a gas with a lower ionization potential for the discharge. This would provide more free electrons for the excitation process. Xe, Kr, or N might be used, or some mixture of gases. The use of a cathode material which has a higher secondary emission coefficient, such as aluminum, should also increase the number of electrons available in the discharge for excitation. The use of aluminum would also contaminate the discharge less, since it is known to have a lower sputtering rate (Ref 1:230).

It is further recommended that the cathode/target geometry be changed so that more uniform sputtering can be achieved. A plane cathode, preferably aluminum, as mentioned previously, should be used. A study should be made to determine if larger diameter electrodes would create more uniform sputtering and more electrons for excitation than the smaller electrodes used in this investigation. It is felt that the electrodes should be water cooled to reduce any chance of increased sputtering rates or sputtering non-uniformity due to heating effects.

After changing the cathode/target geometry, new sputtering rates in GaAs would have to be determined for various discharge parameters.

It is suggested that the GaAs samples used for profiling be capped with a thin metal or other conducting layer after implantation. This should be done in order to allow the sputtering to reach a steady state before the implanted substrate is sputtered.

It is also recommended that larger GaAs samples, on the order of 0.5 to 1.0 cm<sup>2</sup>, be used in order to increase the number of the desired ions in the discharge,

It is recommended that an additional monochromator be used in the experiment. The primary one would be used to monitor the impurity emission line while a second one would be used to monitor the gallium emission line of the GaAs sample being sputtered. Since the emission intensity of the gallium emission line, corresponding to the GaAs substrate, has been shown to be a good indicator of the sputtering rate, this would allow precise monitoring of the target sputtering rate variations during profiling.

Finally, an alternate source of positive ions should be considered for sputtering if uniform sputtering in the GDOS system can not be achieved any other way. The use of the ion gun would provide uniform and controllable sputtering of the sample in the glow discharge.

### Bibliography

1. Cobine, J. D. Gaseous Conductors. New York: Dover Publications, Inc., 1958.
2. Comas, J. and C. B. Cooper. "Ejection Patterns in Low-Energy Sputtering of GaAs and GaP Crystals." Journal of Applied Physics, 39: 5736-5739 (November 1968).
3. ----- "Mass-Spectrometric Study of Sputtering of Single Crystals of GaAs by Low-Energy Ar Ions." Journal of Applied Physics, 38: 2956-2960 (June 1967).
4. Cooper, C. B., R. G. Hart, and J. C. Riley. "Low-Energy Sputtering Yield of the (111) and ( $\bar{1}\bar{1}\bar{1}$ ) Faces of GaAs." Journal of Applied Physics, 44: 5183-5184 (November 1973).
5. Crowder, B. L. "The Influence of the Amorphous Phase on Ion Distributions and Annealing Behavior of Group III and Group V Ions Implanted into Silicon." Electrochemical Society Journal, 118: 947-948 (June 1971).
6. Eisen, F. H. and L. T. Chadderton. Ion Implantation. New York: Gordon and Breach Science Publishers, 1971.
7. Engel, A. V. Ionized Gases. (Second Edition). Oxford: Clarendon Press, 1965.
8. Gibbons, J. F. "Ion Implantation in Semiconductors- Part I: Range Distribution Theory and Experiments." Institute of Electrical and Electronics Engineers Proceedings, 55: 295-319 (March 1968).
9. Gibbons, J. F., W. S. Johnson, and S. W. Mylrcie. Projected Range Statistics. (Second Edition). Stroudsburg, Pennsylvania: Halsted Press, 1975.
10. Green, J. E., F. Sequeda-Osorio, and B. R. Natarajan. "Glow Discharge Optical Spectroscopy as an Analytical Depth Profiling Technique." Journal of Vacuum Science and Technology, 12: 366-369 (January-February 1975).
11. ----- "Glow Discharge Optical Spectroscopy for Micro-volume Elemental Analysis." Journal of Applied Physics, 46: 2701-2709 (June 1975).
12. Green, J. E. and J. M. Whelan. "Glow-Discharge Optical Spectroscopy for the Analysis of Thin Films." Journal of Applied Physics, 44: 2509-2513 (June 1973).

13. Handbook of Chemistry and Physics. (55th Edition).  
Cleveland, Ohio: Chemical Rubber Company Press, 1974.
14. Hippel, A. V. "Kathodenzerstärungs Probleme." Annalen der Physik, 80: 672-707 (1926).
15. Kaminsky, M. Atomic and Ionic Impact Phenomena on Metal Surfaces. New York: Academic Press, Inc., 1965.
16. Kayser, H. Tabelle der Hauptlinien der Linienspektren aller Elemente. Berlin: Verlag von Julius Springer, 1939.
17. Liebl, H. "Secondary-Ion Mass Spectroscopy and its Use in Depth Profiling." Journal of Vacuum Science & Technology, 12: 385-391 (January/February 1975).
18. Linhard, J., M. Scharff, and H. Schiott. "Range Concepts and Heavy Ion Ranges." Kongelige Danske Videnskabernes Selskab, Matematisk-Fysiske Meddelelser, 33: 1-39 (1963).
19. Loeb, L. B. Fundamental Processes of Electrical Discharge in Gases. New York: John Wiley and Sons, Inc., 1939.
20. Marcyk, G. T. "Glow Discharge Optical Spectroscopy For Measurement of Boron Implanted Distributions in Silicon." University of Illinois, Urbana, Illinois: Unpublished Thesis (March 1976).
21. Mayer, J. W. L. Eriksson, and J. A. Davies. Ion Implantation in Semi-conductors. New York: Academic Press, 1970.
22. Papoular, R. Electrical Phenomena in Gases. New York: American Elsevier Publishing Co. Inc., 1965.
23. Pearce, R. W. B. and A. G. Gaydon. The Identification of Molecular Spectra. (Second Edition). New York: John Wiley and Sons, Inc., 1950.
24. Pearmain, K. and B. A. Unvala. "Sputtering of Silicon and Gallium Arsenide with Medium Energy Intense Ion Beams of Argon and Xenon." Vacuum, 25: 3-7 (1975).
25. Stuart, R. V. and G. K. Wehner. "Energy Distribution of Sputtered Cu Atoms." Journal of Applied Physics, 35: 1819-1824 (June 1964).

26. Stuart, R. V. and G. K. Wehner. "Sputtering Yields at Very Low Bombarding Ion Energies." Journal of Applied Physics, 33: 2345-2352 (July 1962).
27. Tables of Spectral Line Intensities. National Bureau of Standards (U.S.) Monograph Number 32 (U.S. GPO, Washington, D. C., 1961), part I.
28. Tisone, T. C. and P. D. Cruzan. "Low-Voltage Triode Sputtering With a Confined Plasma: Part V-Application to Backsputter Definition." Journal of Vacuum Science and Technology, 12: 679 (May/June 1975).

### Vita

David Shelly Hake was born on 20 January 1947 in Lock Haven, Pennsylvania. In June 1964, he graduated from Lock Haven High School and until 1966, attended Lock Haven State College, also located in Lock Haven. He transferred to the University of New Mexico in Albuquerque, New Mexico, from which he received the degree of Bachelor of Science in Physics, in 1968. He entered the OTS program in February 1969 and was commissioned as a Second Lieutenant on 31 March 1969. He then completed pilot training, receiving his wings in April 1970. After pilot training, he served two separate tours with the 963rd and 964th Airborne Early Warning and Control Squadrons, then based at McClellan AFB, California. Between these tours, he served as an EC-47 aircraft commander at Da Nang AB in Vietnam and Nakhon Phanom AB in Thailand from December 1971 until December 1972. He received a regular commission in December 1973 while at McClellan AFB. In May 1975, he departed McClellan AFB, where he was flying with the 964th AEW & C Squadron as an aircraft commander, to enter the School of Engineering, Air Force Institute of Technology in June 1975.

Permanent address: 415 Frederick Street  
Flemington, Pennsylvania 17745

Unclassified

SECURITY CLASSIFICATION OF THIS PAGE (When Data Entered)

REPORT DOCUMENTATION PAGE		READ INSTRUCTIONS BEFORE COMPLETING FORM
1. REPORT NUMBER <b>14</b> GEP/PH/76D-5	2. GOVT ACCESSION NO.	3. RECIPIENT'S CATALOG NUMBER
4. TITLE (and Subtitle) <b>6</b> ION IMPLANTATION IMPURITY ANALYSIS BY GLOW DISCHARGE OPTICAL SPECTROSCOPY		5. TYPE OF REPORT & PERIOD COVERED MS Thesis
7. AUTHOR(s) <b>10</b> David S. Hake Captain USAF		6. PERFORMING ORG. REPORT NUMBER
9. PERFORMING ORGANIZATION NAME AND ADDRESS Air Force Institute of Technology (AFIT-EN) Wright-Patterson AFB, Ohio 45433		8. CONTRACT OR GRANT NUMBER(s) <b>9</b> Master's thesis,
11. CONTROLLING OFFICE NAME AND ADDRESS Electronics Research Branch (AFAL/DHR) Air Force Avionics Laboratory Wright-Patterson AFB, Ohio 45433		10. PROGRAM ELEMENT, PROJECT, TASK AREA & WORK UNIT NUMBERS Project 2306R2-13 <i>Quest not listed</i>
14. MONITORING AGENCY NAME & ADDRESS (if different from Controlling Office) <b>11</b> Dec 76		12. REPORT DATE December, 1976
<b>12</b> 84p.		13. NUMBER OF PAGES 73
16. DISTRIBUTION STATEMENT (of this Report) Approved for public release; distribution unlimited		15. SECURITY CLASS. (of this report) Unclassified
17. DISTRIBUTION STATEMENT (of the abstract entered in Block 20, if different from Report)		15a. DECLASSIFICATION/DOWNGRADING SCHEDULE
18. SUPPLEMENTARY NOTES <i>Jerral F. Guess</i> Approved for public release; IAW AFR 190-17 JERRAL F. GUESS, Captain, USAF Director of Information		
19. KEY WORDS (Continue on reverse side if necessary and identify by block number) Glow Discharge Optical Spectroscopy Gallium Arsenide Ion Implantation Impurity Analysis		
20. ABSTRACT (Continue on reverse side if necessary and identify by block number) The Glow Discharge Optical Spectroscopy technique was investigated to determine if it could be used to measure total impurity concentration profiles in unannealed ion implanted GaAs. Cadmium, zinc, and magnesium ions, which are common p-type dopants in GaAs, were implanted at energies of 99 keV and 120 keV and fluences ranging from $10^{14}$ to $10^{16}$ ions/cm <sup>2</sup> . The implanted GaAs samples were sputtered in a low pressure dc glow discharge <i>10 to the 14th power</i> <i>59 cm</i> <i>next page</i>		

DD FORM 1 JAN 73 1473 EDITION OF 1 NOV 65 IS OBSOLETE

Unclassified

SECURITY CLASSIFICATION OF THIS PAGE (When Data Entered)

10 to the 16th power

012225  
YB

Unclassified

SECURITY CLASSIFICATION OF THIS PAGE(When Data Entered)

20. Continued

→ using argon gas. Intensity of a strong emission line, characteristic of the implanted impurity, was monitored as a function of time. This intensity was combined with independently measured GaAs substrate sputtering rates to calculate total impurity concentration profiles. Uncalibrated concentration profiles were obtained for Zn and Mg in GaAs. None was obtained for Cd.



Unclassified

SECURITY CLASSIFICATION OF THIS PAGE(When Data Entered)